Engineering Science and Technology, an International Journal 43 (2023) 101436

HOSTED BY

Contents lists available at ScienceDirect

Engineering Science and Technology, an International Journal

journal homepage: www.elsevier.com/locate/jestch

Review

Hotspots in maximum power point tracking algorithms for photovoltaic systems – A comprehensive and comparative review

Cem Recai Çırak [a,b,*], Hüseyin Çalık [c]

[a] Department of Electrical and Electronics Engineering, Istanbul University - Cerrahpaşa, Istanbul 34320, Türkiye
[b] Department of Control and Automation Engineering, Istanbul Technical University, Istanbul 34469, Türkiye
[c] Department of Electrical and Electronics Engineering, Giresun University, Giresun 28200, Türkiye

ARTICLE INFO

Article history:
Received 21 January 2023
Revised 27 March 2023
Accepted 6 May 2023
Available online 1 June 2023

Keywords:
Maximum power point tracking
Solar power generation
Photovoltaic systems
Artificial intelligence
Metaheuristics

ABSTRACT

Increasing global energy consumption also raised concerns about environmental issues. Solar energy is one of the most promising sustainable solutions for this problem. However, due to the dynamic behavior of environmental conditions, energy conversion efficiencies of Solar photovoltaic systems decrease considerably. Therefore, to extract the highest energy from photovoltaic systems, the use of maximum power point tracking methods is a necessity. Under partial shading conditions where local maximum power points also occur, global maximum power point tracking is required. In this study, fundamental concepts for photovoltaic systems, conventional maximum power point tracking methods, modern maximum power point tracking methods – which can perform global optimization under partial shading conditions – based on automatic control and artificial intelligence approaches, and advantages and disadvantages of all these methods are provided briefly. Also, a comprehensive review, including more than a hundred prestigious studies carried out on these methods in the last decade is presented categorically and chronologically. Further, discussion and evaluation of reviewed methods in various aspects are given in a nutshell. This study aims to be a guide that may be useful for interested consumers, producers, and researchers and shed light on the last decade of maximum power point tracking methods for photovoltaic systems.

Contents

1. Introduction . . . 2
2. Solar photovoltaic systems . . . 2
   2.1. Solar photovoltaic cell model . . . 3
   2.2. Operation under partial shading condition . . . 4
   2.3. Maximum power point tracking in photovoltaic systems . . . 5
3. Conventional maximum power point tracking methods . . . 6
   3.1. Perturb-and-Observe algorithm . . . 7
   3.2. Incremental conductance algorithm. . . . 7
   3.3. Hill climbing algorithm. . . . 7
   3.4. Fractional Open-Circuit voltage and Short-Circuit current methods . . . 9

Abbreviations: PV, photovoltaic; MPP/GMPP, maximum power point/global maximum power point; MPPT/GMPPT, MPP tracking/GMPP tracking; I-V/P-V, current-voltage/power-voltage; PS/PSC, partial shading/partial shading condition; STC, standard test condition; SS, steady-state; P&O, perturb-and-observe; InC, incremental conductance; HC, hill climbing; FOV/FSC, fractional open-circuit voltage/fractional short-circuit current; FLC, fuzzy logic control; ANFIS, adaptive neuro-fuzzy inference system; ACS, automatic control system; PID/FOPID, proportional-integral-derivative/fractional order PID; SMC, sliding-mode control; AI, artificial intelligence; ANN, artificial neural network; GA, genetic algorithm; SI, swarm intelligence; ACO, ant colony optimization; PSO, particle swarm optimization; ABC, artificial bee colony; FA, firefly algorithm; GSO, glowworm swarm optimization; CS, cuckoo search; GSA, gravitational search algorithm; BA, bat-inspired algorithm; FWA, fireworks algorithm; GWO, grey wolf optimizer; WOA, whale optimization algorithm; SSA, salp swarm algorithm.

* Corresponding author.
E-mail addresses: turkmavisi@ieee.org (C.R. Çırak), huseyin.calik@giresun.edu.tr (H. Çalık).

https://doi.org/10.1016/j.jestch.2023.101436
2215-0986/

4. Modern maximum power point tracking methods . . . 10
4.1. Fuzzy logic control . . . 10
4.2. Automatic control system approaches . . . 10
4.2.1. Proportional-Integral-Derivative control . . . 11
4.2.2. Sliding-mode control . . . 11
4.3. Artificial Neural Network . . . 13
4.4. Genetic algorithm . . . 13
4.5. Swarm intelligence algorithms . . . 13
4.5.1. Ant Colony optimization . . . 14
4.5.2. Particle swarm optimization . . . 15
4.5.3. Artificial bee colony . . . 15
4.5.4. Firefly algorithm . . . 16
4.5.5. Other swarm intelligence algorithms . . . 16
5. Discussion . . . 17
5.1. Conventional MPPT methods . . . 17
5.1.1. Perturbative methods . . . 17
5.1.2. FOV and FSC methods . . . 17
5.2. Modern MPPT methods . . . 17
5.2.1. ACS-based methods . . . 17
5.2.2. AI-based methods . . . 19
5.3. General evaluation of MPPT methods . . . 20
6. Conclusion . . . 20
Declaration of competing interest . . . 21
References . . . 21

1. Introduction

With the effects of the world population, which has increased by 50% during the last three decades and growth in the production sector, electrical energy consumption has followed a continuous upward trend. While the total global electrical energy consumption was at the level of 10.9 PWh in 1990 [1], it has reached 24.7 PWh level by the year 2021 [2]. Due to the sustainability issue that arose with the rapidly increasing demand for electrical energy and the environmental awareness that has increased by the last half-century, the use of alternative renewable energy resources in the production of electrical energy has gained more importance. As from the signing of the Kyoto Protocol in 2005, the amount of electrical energy which is generated from renewable energy resources has started to rise rapidly. While wind and Solar power generation, which constitutes 77% of renewable electrical energy generation, except hydropower, was only around 33.3 TWh in 2000; increasing by more than 50 times in the last two decades, it has reached to 2.9 PWh by 2021, and its share in total electrical energy production has changed from 1.4% to 13.2% [1,2]. As of 2010, the highest increase in renewable electrical energy production is recorded in Solar energy [2].

The modular structure of the Solar photovoltaic (PV) systems enables the use of these systems in various sized applications, which ranges from Solar power generation facilities to the small domestic applications. By extension, with competitive efforts to reduce the costs in Solar PV technologies and the increase in the number of global Solar PV module providers, it is expected that the modules will get significantly cheaper. Hence, it is foreseen that Solar PV systems will continue being a fast-growing renewable electrical energy generation technology in the upcoming three decades [2]. During this process, in connection with the Solar PV systems, there exist substantial and challenging issues, such as the development of Solar cell manufacturing technologies, provision of continual maximum power transfer, and the smart storage of the generated electrical energy.

Improvement of Solar cell manufacturing technologies is an important and developing research topic for material science and chemical engineering. Smart energy storage has become a novel and one of the most promising concepts in the energy management field, particularly the increasing trend to renewable energy systems. On the other hand, maximum power transfer is a well-studied research topic in renewable energy technologies, especially Solar PV systems.

For Solar PV systems, lots of methods called maximum power point tracking (MPPT) to track the maximum achievable power via the system and to transfer the generated power into the load with maximum efficiency have been introduced and developed in a few decades. In this study, a comprehensive review of MPPT methodologies, which have been developed and used in the last two decades, will be presented. First, in Section 2, information about Solar PV systems will be provided in brief. Then, a review of conventional MPPT methods widely used during the last two decades will be given in Section 3. Later on, in Section 4, various modern MPPT methods, including relatively complex control and optimization algorithms that can handle certain issues of conventional MPPT methods, will be presented and reviewed. In further, the overall evaluation and interpretation of MPPT methodologies covered in this study will be discussed in Section 5. Finally, the conclusion will brief the main contributions of this study in Section 6.

2. Solar photovoltaic systems

The performance of Solar PV systems highly depends on both external and internal factors. To utilize a PV system effectively, at first, current–voltage (I-V) characteristics of the system should be well-determined both theoretically and practically, and this requires good mathematical modeling for the system. Robustness of performance of a PV system under rapidly changing environmental conditions like partial shading (PS) is another critical issue. To deal with this issue, global maximum power point tracking (GMPPT) algorithms that can perform global optimization for the best operating point of the PV system have been developed. In this section, fundamentals about PV systems and MPPT methods are introduced. At first, a generic mathematical Solar PV model is provided in Section 2.1. Then, the concept of operation under partial shading condition (PSC) and basics of maximum power point tracking in PV systems are covered in brief under Section 2.2 and Section 2.3, respectively.

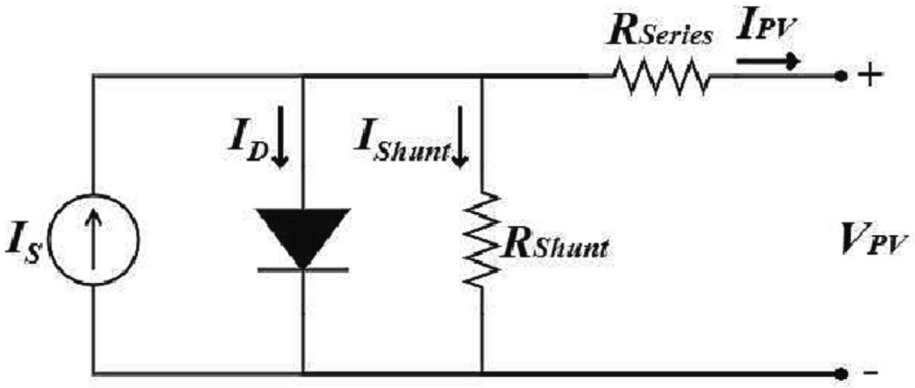

Fig. 1. Solar PV cell model.

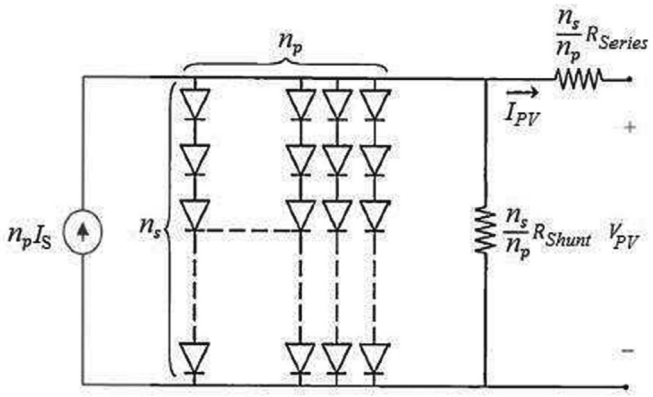

Fig. 2. Solar PV array model connected in series and parallel [10].

2.1. Solar photovoltaic cell model

Solar PV cells produce electrical energy based on a semiconductor with a p-n junction, which is like the diode concept [3]. When a Solar PV cell exposes to Solar radiation, incident photons are absorbed by the junction. Since the absorbed photons transfer their energy to the electrons on the valance band, the energized electrons start to move freely, and thereby this movement leads to DC flow when an external load is connected. Thus, a generic model for a PV cell may simply be represented by using a current source paralleled with a diode and two resistors that one is shunt and the other is connected in series. A generic Solar PV cell model is given in Fig. 1.

For the PV cell model shown in Fig. 1, the output current of the PV cell I_{PV} is expressed in (1) in terms of the diode current I_D, the current through the shunt resistor I_{Shunt} and the current generated by absorbed photons I_S [4].

$$I_{PV} = I_S - I_D - I_{Shunt} \tag{1}$$

where V_{PV} is the output voltage of the PV cell, I_0 is the saturation current of diode, α is ideality factor of the diode, R_{Shunt} is the shunt resistance, R_{Series} is the series resistance, T is the absolute temperature in K, q is the elementary charge, and k is the Boltzmann's constant; I_D and I_{Shunt} are given by (2) and (3) respectively.

$$I_D = I_0 \left[e^{\frac{qV_{PV} + R_{Series} I_{PV}}{\alpha k T}} - 1 \right] \tag{2}$$

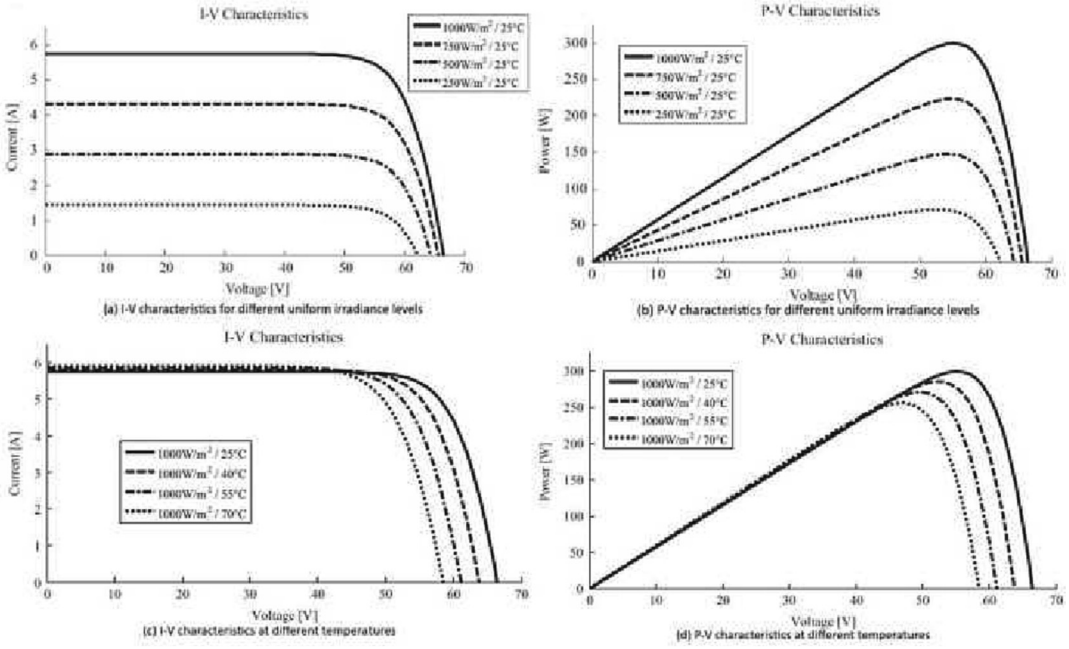

Fig. 3. Typical I-V and P-V characteristics of Solar PV array [3].

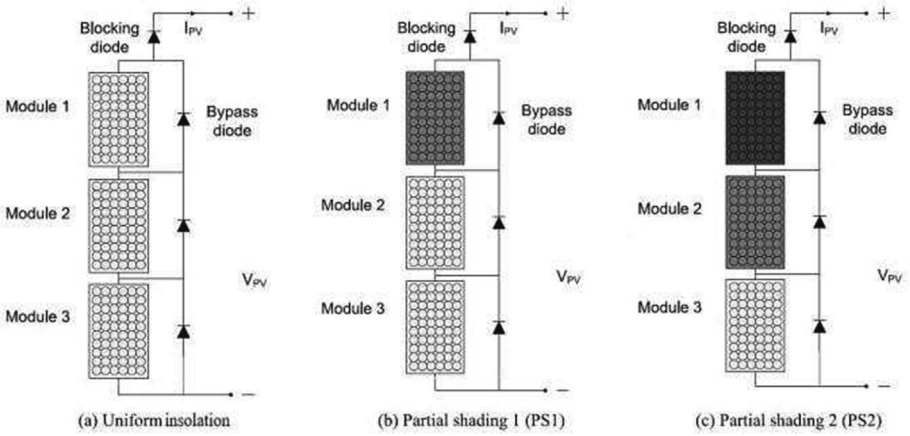

Fig. 4. Solar PV array under uniform insolation and different PS patterns [15].

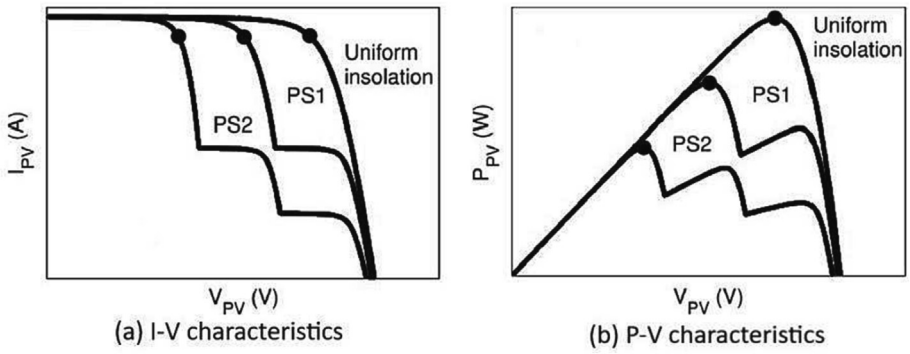

Fig. 5. Solar PV array output I-V and P-V characteristics for the corresponding conditions in Fig. 4.

$$I_{Shunt} = \frac{V_{PV}+R_{Series}I_{PV}}{R_{Shunt}} \tag{3}$$

When (2) and (3) are substituted into (1), I-V characteristic of a PV cell can be represented as in (4) [5,6].

$$I_{PV} = I_S - I_0\left[e^{\frac{q(V_{PV}+R_{Series}I_{PV})}{\alpha kT}} - 1\right] - \frac{V_{PV}+R_{Series}I_{PV}}{R_{Shunt}} \tag{4}$$

Equation (5) provides an expression for the current generated by absorbed photons in terms of Solar irradiance on the surface of PV cell S and temperature T where $I_{S,STC}$, S_{STC} and T_{STC} denote the values of the same parameters in standard test conditions (STC) as $S_{STC} = 1000W/m^2$, $T_{STC} = 298K$, air mass is AM1.5, and K_T represents the temperature coefficient for the short-circuit current of the PV cell [5,6].

$$I_S = \frac{S}{S_{STC}}(I_{S,STC} + K_T(T - T_{STC})) \tag{5}$$

As it is seen from (4) and (5) an increase in Solar radiation level directly leads to an increase in the short-circuit current of the PV cell and maximum output power level as well. However, an increase in temperature causes a major decrease in the open-circuit voltage of the PV cell while it is slightly increasing the short-circuit current, and it leads to a decrease in the maximum output power level [6].

In Solar PV systems, PV modules are combined and configured in compliance with the desired system output as regarding the requirement of the application. PV modules may be combined as a PV array with series and/or parallel connections where parallel connected cells increase output current, and series connected cells increase the output voltage. An expression for the I-V characteristic of a Solar PV array, where n_S and n_P respectively denote the numbers of series and parallel connected PV modules, is given by (6) [4,7]–[9]. PV array model, and I-V and power-voltage (P-V) characteristics for the PV array are given in Fig. 2 and Fig. 3.

$$I_{PV} = n_P\left(I_S - I_0\left[e^{\frac{q\left(V_{PV}+\frac{n_S}{n_P}R_{Series}I_{PV}\right)}{n_S\alpha kT}} - 1\right]\right) - \frac{\frac{n_P}{n_S}V_{PV}+R_{Series}I_{PV}}{R_{Shunt}} \tag{6}$$

2.2. Operation under partial shading condition

Partial shading condition refers to the case that a Solar PV module is exposed to nonuniform irradiation levels due to different shading levels on different cells in the PV array [6,10]. Shading may stem from a cloud, fallen leaves on the PV module, or any obstacle such as tree or building depending on the direction of Sunlight. In a shaded PV cell, which gets no or low irradiation, the photon current decreases as shown in (5). The other cells connected in series with the shaded PV cell compensate for the decreasing photon current by forcing the internal diode of the shaded cell to operate in the avalanche breakdown region. This situation leads that the shaded cell acts as a load and consumes the generated power internally [7,11]. Consumed power may also cause irreversible damage to the shaded PV cell due to the increasing temperature [12,13]. To overcome these issues, and protect the PV module, bypass diodes seen as Fig. 4 are connected in parallel with each PV cell in the array. The shaded PV cell, which acts as load, can be shorted via the bypass diode under PSC. Thus, further voltage-drop at the output and power consumption in the cell is prevented, and the PV module is protected. Also, a blocking diode is connected at the end of each series branch of the PV array to pre-

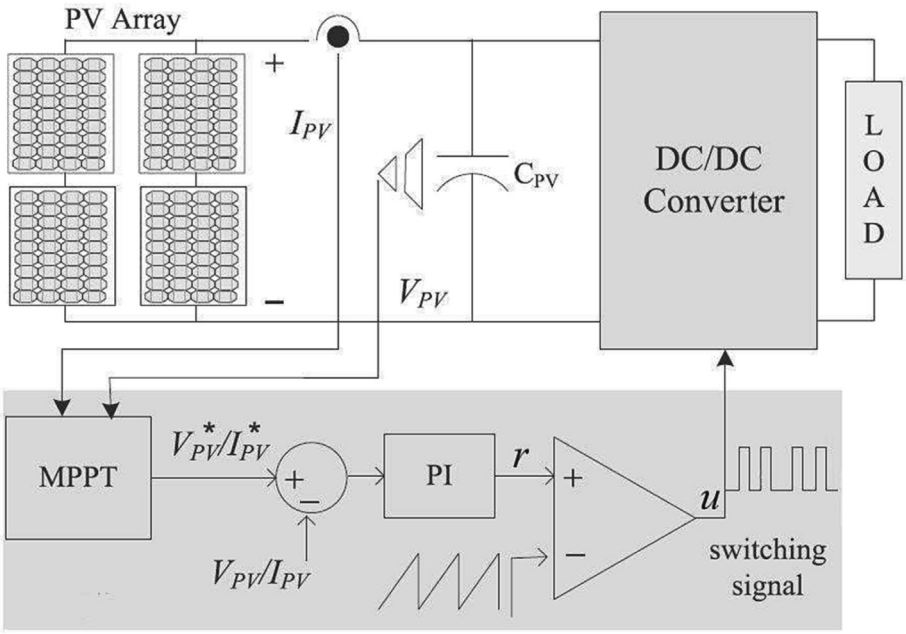

Fig. 6. Solar PV system with MPPT controller [7].

vent the reverse current, which is created by the unbalanced voltage levels between the parallel branches.

Under PSC, bypass diodes lead to a stepped decrease in output I-V curve, and therewith, multiple local maxima and one global maximum power point (GMPP) occur in the output P-V curve of the PV array. Without bypass diodes, these local maxima are not created, and only a single MPP occurs at a level lower than the preceding case [7,14]. In actual applications, only one bypass diode may be added across to a group of PV cells connected in series based on economic reasons. However, in this case, the maximum achievable output power decreases under PSC in comparison to the case that bypass diodes are used for each PV cell. In Fig. 4 and Fig. 5, Solar PV arrays that operate under uniform and different PS patterns, and corresponding output I-V and P-V characteristics for these PV arrays are presented respectively.

2.3. Maximum power point tracking in photovoltaic systems

For obtaining the power with the maximum overall efficiency from a PV system, its operating point must be adjusted as matching the maximum power point (MPP) on its I-V characteristic curve. The overall efficiency for a Solar PV system η is defined as the ratio of average output power $P_{PV,avg}$ to maximum achievable power $P_{PV,max}$ as shown in (7)[11].

$$\eta = 100\frac{P_{PV,avg}}{P_{PV,max}}\% \tag{7}$$

The operating point of a Solar PV system is determined by the intersection point of the I-V characteristic curve of the Solar PV system and the I-V characteristic line of a load which is connected to the PV system. I-V characteristic curve of the PV system depends on atmospheric conditions such as Solar irradiance and temperature, and the slope of a load line changes inversely proportional to the load resistance. Thus, the operating point of the PV system may be shifted with respect to the changes in the slope of load line or atmospheric conditions. Therefore, MPP may be coupled with the operating point of the PV system by changing either load resistance or atmospheric conditions.

Since changing the atmospheric conditions or the load connected to the PV system is not solely viable for real case applications, compulsorily, a DC-DC power converter is used to link the load to the PV module. This converter enables to change the load resistance, which is seen on the PV module side, and consequently

Table 1
P&O general decision process.

ΔV_n	$\Delta P_{PV,n}$	$V_{out,n}$
$\Delta V_n > 0$	$\Delta P_{PV,n} > 0$	Increase by $\lvert\Delta V_{n+1}\rvert$
$\Delta V_n > 0$	$\Delta P_{PV,n} < 0$	Decrease by $\lvert\Delta V_{n+1}\rvert$
$\Delta V_n < 0$	$\Delta P_{PV,n} > 0$	Decrease by $\lvert\Delta V_{n+1}\rvert$
$\Delta V_n < 0$	$\Delta P_{PV,n} < 0$	Increase by $\lvert\Delta V_{n+1}\rvert$

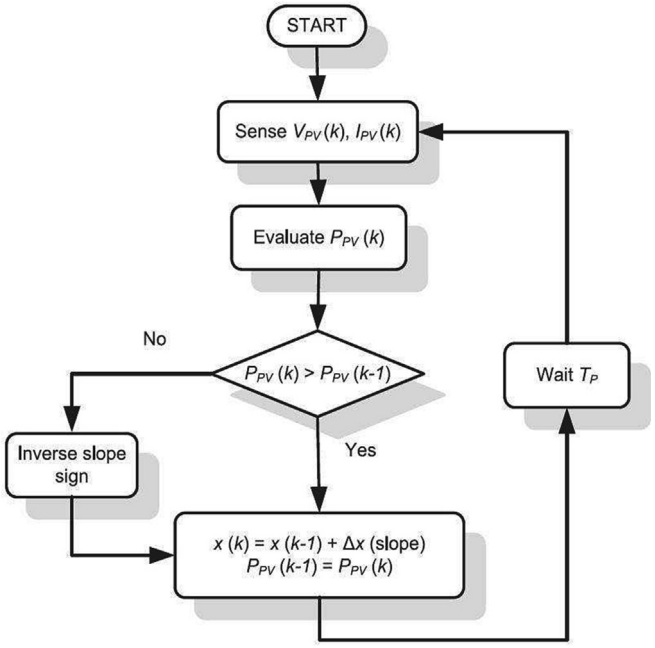

Fig. 7. General P&O MPPT algorithm flowchart [15].

Table 2
Literature review on P&O MPPT algorithm.

Author(s)	Year	Method	Control Variable	Converter/ Processor	Application/Test(s)	Notes and Results
Abdelsalam et al. [17]	2011	Adaptive PI controlled P&O	Duty cycle	Boost converter/ DSP	Standalone system/ Prototype	Minimized SS errors via adapting step sizes by a proportional-integral (PI) controller.
Elgendy et al. [18]	2012	P&O with fixed step-size	Voltage, Duty cycle	Buck converter/ DSP	Standalone system/ Simulation, Water supply system	Duty cycle control worked more stable than voltage control. Obtained 97.9% SS efficiency under rapidly changing irradiance levels.
Ishaque et al. [19]	2014	P&O with fixed step-size	Duty cycle	Buck-boost converter/ DSP	Standalone system/ Prototype	Compared with InC algorithm. InC performed slightly better than P&O with 98.5% to 98.3% SS efficiencies. They fell below 95% under lower irradiation levels.
Mohd Zainuri et al. [20]	2014	Adaptive P&O with FLC	Duty cycle	Boost converter/ DSP	Standalone system/ Simulation, Prototype	Obtained significantly higher efficiencies than sole P&O and FLC, particularly, under low irradiation levels. Traditional P&O efficiency increased by 5%.
Kollimalla and Mishra [21]	2014	Adaptive P&O	Current	Boost converter/ Computer	Standalone system/ Hardware simulation	Chosen step-size based on estimated initial MPP via short-circuit current. Performed faster than traditional P&O.
Killi and Samanta [22]	2015	Drift-free P&O	Duty cycle	Single-ended primary-inductance converter (SEPIC)/μCU	Standalone system/ Simulation, Prototype	Utilized PV current changes to avoid drift issues in traditional P&O due to false decisions under rapid irradiance changes. Overall efficiency increased.
Ahmed and Salam [23–25]	2015, 2016, 2018	Adaptive P&O	Duty cycle	Buck-boost converter/ DSP	Standalone system/ Simulation, Prototype	Shortened step-sizes around MPP according to thresholds based on P-V slope. Reached 99% SS efficiency under fast irradiance changes, 12% higher than traditional P&O.
Alik and Jusoh [26]	2017	Modified P&O with checking algorithm	Duty cycle	Boost converter	Standalone system/ Simulation	Compared all MPPs to identify the GMPP. Adapted step-sizes by a constant scaling factor. Able to perform under PSC.
Ali et al. [27]	2018	Modified P&O with variable step-size	Duty cycle	Boost converter, Inverter	Grid-connected system/ Simulation	Divided the P-V curve into 4 operating regions to adjust step-sizes in MPP adjacencies. SS efficiency increased from 92.6% to 95.4%. Provided a grid connection scheme.
Abdel-Salam et al. [28]	2018	Modified P&O	Duty cycle	Boost converter	Standalone system/ Simulation	Used calculated changes in voltage, current and power together. Obtained 99.48% and 98.03 SS efficiencies under constant and dynamical conditions.
Kamran et al. [29]	2018	Modified P&O	Duty cycle	Boost converter/ μCU	Standalone system/ Simulation, Prototype	An initial search was used to narrow the MPP search region. Tracking speed and overall performance was increased.
Raiker et al. [30]	2021	Momentum-based P&O	Current	Boost converter/ μCU	Standalone system/ Simulation, Prototype	Employed a momentum term for adaptive step-sizes. With current control, tracking speed was doubled and oscillations decreased by 30%.
Ali and Mohamed [31]	2022	Modified P&O with open-circuit voltage	Duty cycle	Boost converter, Inverter	Grid-connected system/ Simulation	Added open-circuit voltage estimations based on measured temperature and STC to [27]. Obtained 99.7% SS tracking efficiency for a 10-hour irradiance profile.

to adjust the operating point of the PV system as it matches with the MPP [4]. Load resistance, which is seen on the PV module side, can be altered via DC-DC power converter by changing its duty cycle. Since MPP may shift dynamically, tracking of MPP requires dynamic duty cycle alteration. This issue brings out the necessity of maximum power point tracking algorithms. A Solar PV system with an MPPT controller is illustrated in Fig. 6.

MPPT algorithms may be classified under two main groups as conventional methods and modern methods. Conventional methods refer to simplistic MPPT algorithms, which have been widely used from the beginning, such as Perturb-and-Observe (P&O) and Incremental Conductance (InC), in particular, and also Hill Climbing (HC), Fractional Open-Circuit Voltage (FOV), and Fractional Short-Circuit Current (FSC). Modern methods encompass various progressive MPPT control and optimization algorithms and approaches, including Fuzzy Logic Control (FLC), Automatic Control System (ACS), Artificial Neural Network (ANN), Genetic Algorithm (GA), and Swarm Intelligence (SI) methods including Ant Colony Optimization (ACO), Particle Swarm Optimization (PSO), Artificial Bee Colony (ABC), Firefly Algorithm (FA), and many other recently developed metaheuristic algorithms. Conventional and modern MPPT methods will be reviewed in Section 3 and Section 4 in order. In Section 5, the overall assessment of these methods will be provided.

3. Conventional maximum power point tracking methods

Conventional MPPT methods, which are simplistic algorithms mainly based on perturbative techniques, have been widely used in Solar PV applications and improved through the last two decades. In this sense, conventional methods are well-studied and well-known MPPT algorithms. In this section, conventional MPPT algorithms will be reviewed. Detailed reviews of P&O and InC algorithms, which are the most commonly used conventional methods,

Table 3
InC general decision process.

Condition1	Condition2	$V_{out,n}$
$\Delta V_n \neq 0$	$G_{PV,n} + \Delta G_{PV,n} > 0$	Increase by $\lvert\Delta V_{n+1}\rvert$
	$G_{PV,n} + \Delta G_{PV,n} < 0$	Decrease by $\lvert\Delta V_{n+1}\rvert$
	$G_{PV,n} + \Delta G_{PV,n} = 0$	No Change
$\Delta V_n = 0$	$\Delta I_{PV,n} > 0$	Increase by $\lvert\Delta V_{n+1}\rvert$
	$\Delta I_{PV,n} < 0$	Decrease by $\lvert\Delta V_{n+1}\rvert$
	$\Delta I_{PV,n} = 0$	No Change

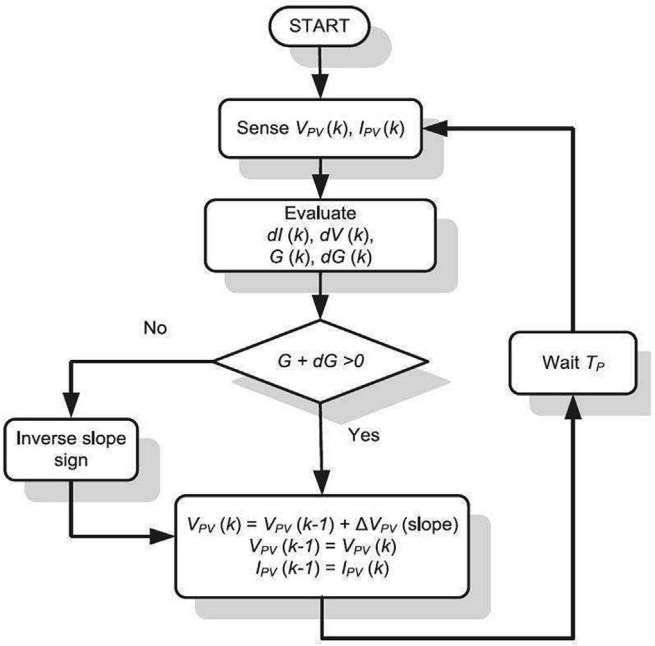

Fig. 8. General InC MPPT algorithm flowchart [15].

will be given in Section 3.1 and Section 3.2 in order. Also, HC algorithm, and FOV and FSC methods will be briefed in Section 3.3 and Section 3.4, respectively.

3.1. Perturb-and-Observe algorithm

Perturb-and-Observe method is the most common MPPT algorithm. In P&O MPPT algorithm, a perturbation is applied on the PV system output voltage at the load side of the DC-DC converter, and the instantaneous output power of the PV array is calculated by multiplying the measured current and voltage values of the PV array. Then, P&O algorithm identifies the direction of the next perturbation step with respect to the perturbation in the PV system output voltage and the change in PV array output power to track MPP. Table 1 briefs the general decision process of P&O MPPT algorithm where ΔV_n is the applied perturbation which has either fixed or variable step-size, ΔP_{PV_n} is the change in PV array power, and $V_{out,n}$ is the PV system output voltage.

The output power of the PV array either increases or decreases based on the output voltage perturbation. Thereby, P&O algorithm continuously tracks the MPP via the output voltage perturbations; thus, the operating point of the PV array oscillates around the adjacency of MPP in the steady-state (SS) [16]. The mathematical expression for P&O MPPT algorithm is provided in (8). Also, the general P&O MPPT algorithm flowchart is shown in Fig. 7.

$$V_{out,n+1} = V_{out,n} + \mathrm{sgn}(\Delta P_{PV,n})|\Delta V_{n+1}| \tag{8}$$

P&O MPPT method shows two major variations with respect to the perturbation step-size as fixed and variable. In P&O algorithm with fixed step-size, the same perturbation size is applied during all tracking process. Smaller step-size decreases the SS error but slows down the tracking speed. Larger step-size increases the tracking speed; however, it also increases the SS oscillations. Therefore, to handle the drawbacks of fixed step-size P&O algorithm, several adaptive or modified P&O variations with variable step-size, which mostly utilize the diminishing perturbations around the MPP, had been developed. Table 2 presents a chronological literature review on P&O MPPT algorithm, including its modified variations.

3.2. Incremental conductance algorithm

Incremental Conductance is another common classical perturbative MPPT algorithm. Similar to P&O MPPT algorithm, in InC MPPT algorithm, a perturbation is applied on the PV system voltage at the DC-DC converter output; instantaneous current and voltage values of the PV array are measured, and changes in these values are calculated. Then, instantaneous conductance of the PV array and change in the conductance are calculated based on the measured current to the voltage of the PV array and calculated changes in them. Since the derivative of PV array output power is directly related to instantaneous conductance and its derivative, decisions for the direction of next perturbation are made based on the comparison of instantaneous conductance and its derivative [7]. The decision process is repeated to approach the MPP. InC MPPT algorithm identifies the MPP where the derivative of PV array output power, and accordingly the sum of instantaneous conductance of PV array G_{PV} with change in the conductance dG_{PV} are zero as per (9) and (10) [15].

$$\frac{dP_{PV}}{dV_{PV}} = \frac{d(V_{PV}I_{PV})}{dV_{PV}} = I_{PV} + V_{PV}\frac{dI_{PV}}{dV_{PV}} = 0 \tag{9}$$

$$\frac{I_{PV}}{V_{PV}} + \frac{dI_{PV}}{dV_{PV}} = G_{PV} + dG_{PV} = 0 \tag{10}$$

Since obtaining the equality condition in (10) is almost impossible for the real cases, instead of exact zero, an interval around zero with a small deviation ε, $(0-\varepsilon, 0+\varepsilon)$, may be used to specify the adjacency of MPP. With this manipulation, a further increase in SS operation performance of InC MPPT algorithm can be achieved. Also, adaptive implementations with variable perturbation step-size can be utilized in InC MPPT method. InC algorithm also can detect the changes in current during the SS operation by comparing calculated changes in output current and voltage values of PV array. Thus, InC algorithm can eliminate the oscillations which occur due to changes in environmental conditions or noises in SS operation. This brings a significant advantage in comparison to the traditional P&O algorithm. The general decision process of InC MPPT algorithm is given in Table 3 where ΔI_{PV_n} and ΔG_{PV_n} are the changes in current and conductance of PV array, respectively. Equation (11) provides the mathematical representation for the InC MPPT algorithm. Also, a flowchart for the general InC MPPT algorithm is shown in Fig. 8. Related works on InC MPPT algorithm and its variations are given in Table 4 in chronological order.

$$V_{out,n+1} = \begin{cases} V_{out,n} + \mathrm{sgn}(\Delta I_{PV,n})|\Delta V_{n+1}|, & \text{if } \Delta V_n = 0 \\ V_{out,n} + \mathrm{sgn}(G_{PV,n} + \Delta G_{PV,n})|\Delta V_{n+1}|, & \text{otherwise} \end{cases} \tag{11}$$

3.3. Hill climbing algorithm

Hill climbing is another common classical MPPT method which is actually a popular variant of P&O. Both algorithms utilize exactly the same perturbative approach, and even sometimes, HC and P&O terms are used interchangeably. As distinct from P&O, in HC algorithm, perturbations are directly applied on the duty cycle which controls the on–off ratio of the DC-DC converter instead of PV sys-

Table 4
Literature review on InC MPPT algorithm.

Author(s)	Year	Method	Control Variable	Converter/Processor	Application/Test(s)	Notes and Results
Safari and Mekhilef [32]	2011	InC with fixed step-size	Duty cycle	Ćuk converter/DSP	Standalone system/Simulation, Prototype	Used a simplified, low-cost circuit design via direct control method. Stated that obtained acceptable responses, but efficiency was not specified.
Mei et al. [33]	2011	Modified InC with variable step-size	Duty cycle	Boost converter/μCU	Standalone system/Simulation, Prototype	Varied step-sizes according to the slope of the PV output power and duty cycle characteristic curve. Provided faster response and less SS error than traditional InC.
Sera et al. [34]	2013	InC and P&O with fixed step-sizes	Voltage	Boost converter, Inverter	Grid-connected system/Simulation	Mathematically analyzed indifference of InC and P&O. Experimentally revealed that there is no statistically significant difference between them. Reached 99% and 95–98% SS efficiencies under constant and changing conditions.
Tey and Mekhilef [35]	2014	Modified InC	Duty cycle	SEPIC/μCU	Standalone system/Simulation, Prototype	Used small intervals instead of a single point for MPP. Outperformed traditional InC in terms of SS oscillations and MPP accuracy.
Radjai et al. [36]	2014	Modified InC with fuzzy logic estimator	Duty cycle	Ćuk converter/DSP	Standalone system/Simulation, Prototype	Changed duty cycles based on a fuzzy logic estimator. Reached 99.6% SS efficiency. Able to perform under PSC and fast irradiance changes.
Sivakumar et al. [37]	2015	Modified InC	Voltage	Buck-boost converter, Inverter/DSP	Grid-connected system/Simulation, Prototype	Utilized PV output currents calculated as a function of load impedance to reduce oscillations due to ripples. Performed with better efficiency than traditional InC.
Putri et al. [38]	2015	InC with fixed step-size	Duty cycle	Buck-boost converter	Standalone system/Simulation	Able to track MPP with higher efficiency and lower SS oscillations but slower responses than P&O under changing conditions.
Loukriz et al. [39]	2016	InC with variable step-size	Duty cycle	Buck-boost converter/ DSP	Standalone system/Simulation, Prototype	Varied step-sizes based on the ratio of change in PV output power to the difference of the changes of PV output voltage and current. Provided faster responses, less oscillations, and higher SS efficiency than traditional InC under fast irradiation changes.
Elgendy et al. [40]	2016	InC with fixed step-size	Voltage, Duty cycle	Buck converter/DSP	Standalone system/Simulation, Water pump system simulation	Examined frequency selection method similarly to [18]. Sped up convergence and increase efficiency with high frequency perturbation and duty cycle control. Obtained 97.4% and 98.8% SS efficiencies under slowly and rapidly changing irradiances.
Zakzouk et al. [41]	2016	Low-cost InC with variable step-size	Duty cycle	Boost converter/μCU	Standalone system/Simulation, Prototype	Exchanged the divisions used for InC algorithm with multiplications and a few additional comparisons. Able to implement in low-cost μCU via reducing required process power. Reached 99.7% and 94.3% SS efficiencies under uniform irradiance and PS.
Kumar et al. [42]	2018	Self-adaptive InC	Duty cycle	Boost converter/CPU	Standalone system/Simulation, Prototype	Adapted step-sizes by estimating MPP region based on PV output power and voltage comparison over moving 3 consecutive points. Rose speed and SS efficiency.
Shahid et al. [43]	2018	Temperature controller and InC	Duty cycle	Boost converter/μCU	Standalone system/Prototype	Used PV cell temperature as an extra input. Adjusted the Fresnel lens angle to optimize PV cell operating temperature and increase maximum achievable power.
Motahhir et al. [44]	2018	Modified InC with variable step-size	Duty cycle	Boost converter	Standalone system/Simulation	Detected sudden irradiance changes based on the ratio of changes in PV output power to output voltage while allowing small oscillations around MPP. Obtained 98.8% SS efficiency under fast changing irradiance levels.
Necaibia et al. [45]	2019	Modified InC	Duty cycle	SEPIC/μCU	Standalone system/Simulation, Prototype	Adapted step-sizes based on the region in or out MPP adjacency. Implemented in low-cost μCU. Reduced SS oscillations and sped up convergence in dynamic conditions.
Mishra et al. [46]	2021	Modified InC with adaptive step-size and frequency	Duty cycle	Boost converter/μCU	Standalone system/Simulation, Prototype	Adapted step-sizes according to change in output voltage and iteration frequencies based on step-size. Significantly reduced SS oscillations via simple low-cost modifications.
Ahmed et al. [47]	2022	InC with ANFIS	Duty cycle	Boost converter	Grid-connected system/Simulation	Used Adaptive Neuro-Fuzzy Inference System (ANFIS) trained via crow and pattern search. Utilized temperature and irradiance data. Outperformed conventional and fuzzy methods with 99% tracking efficiency. Required complex and high-cost modifications.

Table 5
Literature review on HC MPPT algorithm.

Author(s)	Year	Method	Control Variable	Converter/ Processor	Application/Test(s)	Notes and Results
Lohmeier et al. [55]	2011	Current-sensorless HC	Duty cycle	Double-boost converter/ Computer	Standalone system/ Simulation, Prototype	Estimated PV output current based on voltage ripples measured on the converter input. Tested under real weather conditions. Performed with 86%-91% tracking efficiencies.
Kjær [56]	2012	HC and InC with fixed step-sizes	Duty cycle	Boost converter, Inverter/ Computer	Grid-connected system/Hardware simulation	Compared with InC on a grid-connected hardware under 27 real irradiation profiles over a year. Revealed that there is no statistically significant difference at 95% confidence level. Obtained 99.8% SS efficiencies for both algorithms.
Abuzed et al. [53]	2014	Modified HC with variable step-size	Duty cycle	Boost converter/ Computer	Standalone system/ Simulation, Hardware simulation	Adapted step-sizes according to changes in PV output power. Reached 99.4% and 98.8% SS efficiencies under constant and dynamic conditions.
Lasheen and Abdel-Salam [54]	2018	Hybrid HC with ANFIS controller	Duty cycle	Boost converter	Standalone system/ Simulation	Estimated reference duty cycle ratio for MPP by ANFIS controller. Used irradiation, temperature, and PV output current and voltage measures. Responded fast and accurate with higher SS efficiency under both rapid and nonlinear irradiation changes.
Bouakkaz et al. [57]	2020	Modified HC with FLC	Duty cycle	Boost converter	Standalone system/ Simulation	Utilized a FLC to adapt step-sizes based on measured PV output voltage and current. Provided stable output under sudden irradiance and temperature changes.

Table 6
Literature review on FOV and FSC MPPT methods.

Author(s)	Year	Method	Control Variable	Converter/ Processor	Application/Test(s)	Notes and Results
Ahmad [58]	2010	FOV	Voltage	Buck converter/No processor is required	Standalone system/ Prototype	Decreased power losses due to load disconnection during measurements via using short sampling time and period with a timer. Needed no processor. Lowered cost.
Sher et al. [59,60]	2015, 2018	Hybrid FSC with P&O	Duty cycle	Buck-boost converter, Inverter/DSP	Standalone system, Grid-connected system/ Simulation, Hardware simulation	Estimated PV output current for MPP via FSC. Used P&O to fine-tune for actual MPP. Obtained 97.6% and 95.7% SS efficiencies for standalone system and 96.3% and 95.8% efficiencies for grid-connected systems under constant and dynamic conditions.
Hua et al. [61]	2016	Hybrid current-sensorless modified FOV	Duty cycle	Boost converter/DSP	Standalone system/ Simulation, Prototype	Set thresholds for the MPP region via FOV. Applied fine-tuning by InC-like method. Adapted step-sizes based on PV output voltage and duty cycle and changes in them. Reached 99.7% SS efficiency.
Bounechba et al. [62]	2016	FSC with current perturbation	Current	Boost converter/DSP	Standalone system/ Simulation, Hardware simulation	Derived short-circuit currents based on the measured irradiation levels instead of disconnecting PV array. Obtained faster response and less SS oscillations than P&O.
Hmidet et al. [63]	2021	Improved FOV	Duty cycle	Boost converter, Inverter/DSP	Standalone system/Water pump system	Adjusted duty cycle according to comparison of PV voltage and estimated MPP voltage based on measured temperature. Increased tracking speed, accuracy, and efficiency.

tem output voltage [48,49]. As analogous to P&O, in HC algorithm, a perturbation is applied on the duty cycle of the converter, and instantaneous output power of the PV array is calculated as the multiplication of measured instantaneous current and voltage values of the PV array. Then, the direction of the next perturbation step is identified based on the perturbation in the duty cycle and the change in PV array output power.

HC algorithm follows the same decision process with P&O algorithm. If the applied perturbation and the change in the output power of the PV module are in the same direction, then an increment will be applied to the duty cycle. If they are in opposite directions, then the duty cycle will be reduced [50]. The general HC MPPT algorithm can be represented by (12) where $D_{PV,n}$ denotes the duty cycle of the converter and ΔD_n is the fixed or variable perturbation step-size which is applied on duty cycle.

$$D_{PV,n+1} = D_{PV,n} + \mathrm{sgn}(\Delta P_{PV,n})|\Delta D_{n+1}| \quad (12)$$

The main advantage of HC MPPT algorithm is the simplified control via directly applied PWM signal on the converter. The disadvantages of HC method are the same with P&O and InC algorithms. The main drawback of HC algorithm is the SS oscillations which decrease the efficiency during the operation in the adjacency of MPP [51]. For solving this issue, a modified HC algorithm with variable step-size can be employed [52]–[54]. A brief literature review on HC MPPT algorithm is provided in Table 5.

3.4. Fractional Open-Circuit voltage and Short-Circuit current methods

Fractional open-circuit voltage is a simple method that directly sets the operating voltage to a certain fraction of the open-circuit voltage of the PV system. In FOV method, first, the load is disconnected, and the instantaneous open-circuit voltage of the PV system is recorded. Then, measured open-circuit voltage is scaled by optimal proportionality constant and assigned as the operating voltage of the PV system. This procedure is periodically repeated during the operation. FOV method can be applied as given in (13) where V_{PV} is PV output voltage which corresponds to the estimated MPP, K_{OC} is the optimal proportionality constant for the open-circuit coefficient, and V_{OC} denotes the open-circuit voltage of the PV system. In general, K_{OC} is selected between 0.71 and 0.78 [48].

$$V_{PV,MPP} = K_{OC}V_{OC} \quad (13)$$

Fractional short-circuit current method is another simple method which analogous to FOV method. In FSC method, first, the load is shorted, and the instantaneous short-circuit current of the PV system is recorded. Then, measured short-circuit voltage is scaled by optimal proportionality constant and assigned as the operating current of the PV system. This procedure is periodically repeated during the operation. FSC method can be applied as per (14) where $I_{PV,MPP}$ is PV output current which corresponds to the

estimated MPP, K_{SC} is the optimal proportionality coefficient for the short-circuit current, and I_{SC} denotes the short-circuit current of the PV system. Typical values of K_{SC} vary between 0.78 and 0.92 [48].

$$I_{PV,MPP} = K_{SC} I_{SC} \tag{14}$$

FOV and FSC methods are mainly employed for their simplicity. Also, FOV only requires a voltage sensor, and FSC only requires a current sensor as well. Thereby, FOV and FSC methods provide a simple and economical way to control a Solar PV system. Besides their advantages, FOV and FSC methods bring a variety of disadvantages. The main disadvantage of these methods stems from interruptions of power transfer due to periodical shorting or opening the circuit during the sensing actions. Additionally, none of these methods can provide high accuracy MPP tracking. Accuracies get worse under PS and fast changing environmental conditions. All these disadvantages cost to power losses. Therefore, in this manner, FOV and FSC methods can be regarded as an inefficient way to control a PV system. Some of the related works on FOV and FSC MPPT methods are provided in Table 6.

4. Modern maximum power point tracking methods

Modern MPPT methods have been needed to overcome some specific issues about MPP tracking, such as operating under the PS or fast changing irradiance conditions where conventional MPPT methods were not sufficient. Modern MPPT methods actually refer to some Artificial Intelligence (AI) algorithms, and Automatic Control System approaches that are adapted and utilized for MPPT. MPPT algorithms based on Fuzzy Logic Control, Automatic Control System, and Artificial Neural Network methods will be given in Section 4.1, Section 4.2, and Section 4.3, respectively. Also, Genetic Algorithm for MPPT will be provided in Section 4.4. Finally, in Section 4.5, MPPT methods, which utilize various Swarm Intelligence algorithms, will be covered.

4.1. Fuzzy logic control

Fuzzy Logic Control is an AI control algorithm based on some "if statements" that enable constructing nonlinear models. In general, FLC can be preferred due to its robust performance in handling uncertain or unexpected situations by means of its fuzzy modeling instead of exact mathematical expressions [64]. However, FLC algorithm comes with the complexity in the construction of fuzzy membership functions and inference rules based on these functions truly.

FLC algorithm consists of three main stages which are fuzzification, inference rules, and defuzzification. In the fuzzification stage, inputs of the FLC are converted into categorical inputs according to their belongingness to fuzzy membership functions. In the inference rules stage, FLC matches the fuzzified inputs with the corresponding quantized control action based on the prespecified if statements. In the defuzzification stage, the fuzzy control output variable is generated based on the final membership, which calculated by combining all memberships, and this output is converted back into the numerical control output [65]. In general, an FLC-based MPPT algorithm uses an error value e_n and change in the error Δe_n as input variables which may be defined as given in (15) and (16). The output of FLC is usually selected as the duty cycle ratio D_n or change in duty cycle ratio ΔD_n for MPPT applications.

$$e_n = \frac{\Delta P_{PV,n}}{\Delta V_{PV,n}} \tag{15}$$

$$\Delta e_n = e_n - e_{n-1} \tag{16}$$

Both membership functions and inference rules can be defined by the FLC designers depending on either their knowledge or empirical results. An example of typical five different membership functions of which two are right-angled trapezoids in two tails and three are triangles in the middle can be seen in Fig. 9, where LN is large negative, SN is small negative, Z is zero, SP is small positive, and LP is large positive.

Table 7 presents an example of FLC inference rules which are based on membership functions shown in Fig. 9. For instance, if the operating point of the PV system is in the left adjacency of MPP, e_n becomes SN and if Δe_n is Z; then, output ΔD_n will be SN according to rules given in Table 7.

FLC-based MPPT algorithms are rarely used alone. They are highly appropriate for hybridization with other control, search, and optimization techniques which include both conventional and modern MPPT methods. In particular, neuro-fuzzy controllers, which employ an embedded ANN algorithm in FLC system to optimize membership function parameters adaptively, can be used for effective MPP tracking under dynamic conditions. Since ANN can also provide auto-tuning for inference rules, a neuro-fuzzy controller does not require the designer's knowledge. In Table 8, a chronological literature review on FLC-based MPPT algorithms and its hybridized variations is given.

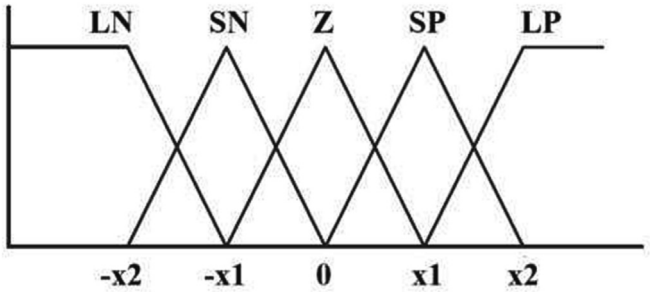

Fig. 9. Membership functions for FLC.

4.2. Automatic control system approaches

Automatic Control Systems basically refer to closed-loop feedback control systems which consist of a plant/actuator, a controller, a sensor, and a comparator/regulator. ACS is used to match the output of a system with the applied reference input. Automatic control approaches may be applied to systems that

Table 7
Inference rules for FLC.

e_n	Δe_n				
	LN	SN	Z	SP	LP
LN	LN	LN	LN	SN	Z
SN	LN	SN	SN	Z	SP
Z	LN	SN	Z	SP	LP
SP	LN	Z	SP	LP	LP
LP	Z	SP	LP	LP	LP

Table 8
Literature review on FLC-based MPPT algorithms.

Author(s)	Year	Method	Control Variable	Converter/ Processor	Application/Test(s)	Notes and Results
Alajmi et al. [66]	2011	FLC-based modified HC	Duty cycle	Boost converter/ DSP	Standalone system/ Simulation, Prototype	Varied step-sizes via FLC for HC. Provided faster MPP convergence and less SS oscillations than traditional HC.
Adly et al. [67]	2011	FLC with FOV	Duty cycle	Boost converter	Standalone system/ Simulation	Employed FOV to estimate MPP. Reduced the MPP convergence time by 20% in comparison to sole FLC.
Nabulsi et al. [68]	2012	FLC-based modified P&O	Duty cycle	Buck converter/ DSP	Standalone system/ Simulation, Prototype	Changed step-sizes by FLC. Tested for 1 h under real weather conditions. Sped up convergence and reduced SS oscillations in comparison to traditional P&O.
Chen et al. [69]	2016	FLC-based adaptive InC	Duty cycle	Boost converter/ DSP	Standalone system/ Simulation, Prototype	Adapted step-sizes by FLC according to slope of P-V curve of PV array. Outperformed fixed step-size InC, adaptive InC, and FLC-based modified HC with 98% SS efficiency.
Al-Majidi et al. [70]	2018	FLC-based modified P&O	Duty cycle	Boost converter, Inverter	Grid-connected system/Simulation	Adjusted step-sizes via FLC for P&O based on the ratios of change in PV output power to output power and to change in output voltage. Reached 99.6% overall efficiency and outperformed sole FLC and P&O.
Hong et al. [71]	2018	PSO-tuned FLC	Duty cycle	Boost converter/ DSP	Standalone system/ Simulation, Prototype	Designed FLC based on a procedure following Taguchi method. Tuned FLC parameters by PSO. Outperformed InC with 96.25% overall efficiency.
Bahrami et al. [72]	2019	Modified FLC	Duty cycle	Boost converter/ DSP	Standalone system/ Simulation, Hardware simulation	Varied step-sizes via FLC estimating MPP region based on PV output power and voltage comparison over moving 3 consecutive points. Employed P&O to reach actual MPP. Outperformed sole P&O and FLC with faster convergence and higher SS efficiency.
Kececioglu et al. [73]	2020	Hybrid modified FLC with InC	Duty cycle	Boost converter/ DSP	Standalone system/ Simulation, Prototype	Modified FLC by using type-2 fuzzy gaussian membership set and hybridizing with angle InC. Outperformed sole InC with 93.3% SS efficiency and 99.8% accuracy.
Bisht and Sikander [74]	2022	Improved FLC	Duty cycle	Boost converter	Standalone system/ Simulation	Used changes in PV input voltage and output power and previously recorded responses for various temperature and irradiance levels as inputs for FLC. Reached 96% accuracy.

are linear or nonlinear. ACS approaches are widely utilized in almost every control action and in MPPT control as well. MPPT methods which are based on the most common ACS approach, Proportional-Integral-Derivative (PID) control, and on a nonlinear ACS approach, Sliding-mode Control (SMC), will be presented in Section 4.2.1 and Section 4.2.2 in order.

4.2.1. Proportional-Integral-Derivative control

Proportional(P)-Integral(I)-Derivative(D) control is the most common control method since 1950 s [75]. A generic PID controller tracks a reference input by generating a control signal as a weighted linear combination of three terms that are proportional to the instantaneous error, the cumulative sum of the errors, and changes in the error, where the error e_n denotes the difference between the reference input $y_{ref,n}$ and the actual output y_n of the control system. PID control also has variations such as P, I, PI, PD, or fractional-order PID (FOPID) that include I and D terms with fractional exponents. The most important part of the PID controller design is selection of parameters K_P, K_I and K_D which are coefficients of P, I and D terms respectively. These parameters can be tuned by using some systematic predetermined rules which are developed based on experiments such as well-known Ziegler-Nichols method [76]. Also, various optimization techniques can be employed for more accurate PID tuning performance [77]. Generic approximate discrete PID controller output c_n can be represented as per (17), where ΔT is the period between two consecutive measurements.

$$c_n = K_P e_n + K_I \sum_{l=1}^{n} e_l \Delta T + K_D \frac{e_n - e_{n-1}}{\Delta T} \tag{17}$$

PID and PI controllers are also utilized as MPPT controllers since it provides more stable SS operation in comparison to classical methods although its initial response speed is relatively low. For MPPT control, the rate of change in PV output power with respect to the PV output voltage is defined as control system output. The reference input of the control system is chosen as zero to reach the MPP, where the slope of the P-V characteristic of the PV module is zero. Therefore, e_n and c_n can be defined as per (18) and (19).

$$e_n = y_{ref,n} - y_n = 0 - \frac{\Delta P_{PV,n}}{\Delta V_{PV,n}} = -I_{PV,n} - V_{PV,n} \frac{\Delta I_{PV,n}}{\Delta V_{PV,n}} \tag{18}$$

$$c_n = -K_P \frac{\Delta P_{PV,n}}{\Delta V_{PV,n}} - K_I \sum_{l=1}^{n} \frac{\Delta P_{PV,l}}{\Delta V_{PV,l}} \Delta T - \frac{K_D}{\Delta T} \left(\frac{\Delta P_{PV,n}}{\Delta V_{PV,n}} - \frac{\Delta P_{PV,n-1}}{\Delta V_{PV,n-1}} \right) \tag{19}$$

4.2.2. Sliding-mode control

Sliding-mode Control is a robust nonlinear control algorithm that is capable of handling nonlinear system models, changing parameters, external disturbances, and uncertainties. SMC is mostly employed to provide robust control under high uncertainties. Therefore, SMC is appropriate to be used in applications where the system model is imprecise [78]. SMC has two different modes which are convergence-mode and sliding-mode. In convergence-mode, the system state approaches a sliding surface with discontinuous movements. In sliding-mode, the system state moves to reference value through the sliding surface [79].

For a system defined by (20) and (21) where u is the control input vector, y is the system output vector, x is the state vector, $e = y_{ref} - y$ is the error between desired output reference and actual output, and $\dot{x}$ and $\dot{e}$ are first derivatives of x and e; a sliding surface σ may be represented as per (22).

$$\dot{x} = Ax + Bu \tag{20}$$

$$y = Cx + Du \tag{21}$$

$$\sigma = f\left(e, \dot{e}, \cdots, e^{(m)}\right) = e^{(m)} + \sum_{l=0}^{m-1} \beta_l e^{(l)} \tag{22}$$

In the first step, an appropriate sliding surface, which diminishes towards zero, is selected. In general, a sliding surface is represented by a parameter α and the derivative order m as shown in (23). In the second step, the control input is selected, simply as given in (24) where k is a positive real number.

Table 9
Literature review on ACS-based MPPT algorithms.

Author(s)	Year	Method	Control Variable	Converter/ Processor	Application/Test(s)	Notes and Results
Dounis et al. [81]	2013	Adaptive FLC-tuned PID	Duty cycle	Buck converter	Standalone system/ Simulation	Tuned PID via FLC adapted by using scaling factors generated by another FLC. Fed the slope of P-V curve back to controller block. Outperformed traditional PID and P&O with 87.3–98.4% SS efficiencies under various conditions.
Levron and Shmilovitz [82]	2013	Dual loop with SMC and P&O	Duty cycle	Boost converter/ DSP	Standalone system/ Hardware simulation	Combined SMC and P&O in dual loop. Generated reference input for SMC by P&O. Defined sliding surface based on input current and voltage of converter and reference. Able to perform under PSC. Reached 93% SS efficiency under changing irradiation.
Bianconi et al. [83]	2013	Current-based P&O with SMC	Duty cycle	Boost converter/ μCU	Grid-connected system/ Simulation, Prototype	Generated reference input for SMC via current-based P&O. Defined sliding surface based on the current sensed through input capacitor of converter, inductor current, and PV output current. Able to perform under fast changing irradiance and PSC.
Mamarelis et al. [84]	2014	P&O-based SMC	Voltage	SEPIC/DSP	Standalone system/ Simulation, Prototype	Generated reference input for SMC by P&O. Theoretically analyzed SEPIC topology and dynamic behavior and stability of system. Verified experimentally.
Kumar et al. [85]	2015	InC-based PID	Duty cycle	Boost converter	Standalone system/ Simulation	Provided reference input based on the difference of the slope of the P-V curve and InC expression given by (9) and (10). Tuned PID via Ziegler-Nichols method. Outperformed P&O and InC. with faster response and 97.4% SS efficiency.
Harrag and Messalti [86]	2015	GA-tuned PID-controlled P&O	Duty cycle	Boost converter	Standalone system/ Simulation	Varied step-sizes by offline GA-tuned PID. Defined error term as difference of PV array and converter output powers. Used P&O to search MPP. Reached 96.7% SS efficiency.
Belkaid et al. [87]	2016	SMC	Duty cycle	Boost converter/ DSP	Standalone system/ Simulation, Hardware simulation	Selected sliding surface as per (26). Utilized converter output voltage as input. Used a smaller step-size in MPP adjacency. Outperformed P&O and InC with, faster and more accurate responses and less SS oscillations.
Montoya et al. [88]	2016	P&O-based SMC	Duty cycle	Boost converter/ DSP	Grid-connected system/ Simulation, Prototype	Defined a sliding surface based on current sensed through converter input capacitor, PV output voltage, and reference voltage provided by P&O. Showed effective MPP tracking and robust performance under disturbance.
Pradhan and Subudhi [89]	2016	FOV-based double integral SMC	Duty cycle	Boost converter/ FPGA	Standalone system/ Simulation, Prototype	Combined double-integral controller with SMC. Defined controller error as difference between reference voltage obtained by FOV and PV output voltage. Selected sliding surface as sum, integral, and double integral of the error. Outperformed P&O, adaptive P&O, SMC, and integral SMC with 99.3% SS efficiency.
Yang et al. [90]	2018	P&O-based FOPID	Duty cycle	Inverter/ DSP	Grid-connected system/ Hardware simulation	Tuned P&O-based FOPID by simple yin-yang-pair optimizer. Fed inverter output current back to controller. Able to find GMPP under PSC. Outperformed PID, FLC, FOPID, and SMC in response time, overshoot, and SS error.
Al-Dhaifallah et al. [91]	2018	InC-based fractional-order I control	Duty cycle	Boost converter	Standalone system/ Simulation	Defined controller error as per (9) and (10). Tuned fractional-order I by PSO based radial movement optimizer. Tracked MPP accurately and sped-up InC by 41.7%.
Nasir et al. [92]	2021	Adaptive FOPID with PSO	Voltage, Current	Inverter	Grid-connected system/ Simulation	Tuned FOPID online via PSO when an error occurred. Reduced total harmonic distortion ratio by 1.9%. Outperformed FOPID, FLC, PI, ACO-based FOPID, and GA-based FOPID with faster convergence and lower overshoot.
Inomoto et al. [93]	2022	Cascade SMC	Current, Duty cycle	Boost converter/ DSP	Standalone system/ Simulation, Hardware simulation	Cascaded voltage and current control loops. Used voltage loop to give reference for current loop. Performed slightly better than SMC-PI, and 2-pole 2-zero controllers in settling time under changing irradiance.

$$\sigma = \left(\frac{d}{dt} + \alpha\right)^m e \tag{23}$$

$$u = k\mathrm{sgn}(\sigma) = \begin{cases} k, \ for \ \sigma > 0 \\ -k, \ for \ \sigma < 0 \end{cases} \tag{24}$$

In SMC, a common drawback called chattering problem is the oscillations in zig-zag shape which occur in SS operation due to discrete switching in control input. For solving this problem, the transition of control input where the sliding surface is close to zero can be smoothed by replacing signum function with a continuous function such as sigmoid or tanh [80]. A smoother control input can be defined as seen in (25).

$$u = k\tanh(\sigma) = \frac{2k}{1+e^{-2\sigma}} - 1 \tag{25}$$

For MPPT control, the sliding surface can be chosen as the rate of change in output power of the PV array with respect to the change in voltage. Thus, MPP is reached when the sliding surface function becomes zero as per (26). Therefore, control input can be selected as the operating voltage of the PV and adjusted by SMC as shown in (27).

$$\sigma_n = \frac{\Delta P_{PV,n}}{\Delta V_{PV,n}} = I_{PV,n} + V_{PV,n}\frac{\Delta I_{PV,n}}{\Delta V_{PV,n}} \tag{26}$$

$$V_{out,n+1} = V_{out,n} + |\Delta V| tanh(\sigma_n) \tag{27}$$

A literature review on ACS-based MPPT algorithms is provided in Table 9 in chronological order.

4.3. Artificial Neural Network

Artificial Neural Networks refer to an AI-based bio-inspired probabilistic modeling technique which was first proposed based on the organization in the human brain by F. Rosenblatt in 1958 [94]. ANN is mostly employed for modeling processes which have complex and nonlinear structure via simply mimicking working principle of the neurons in the human brain. Thus, ANN is able to solve more complex problems by developing its knowledge, which is learned in the training process, based on previous data. A typical ANN structure consists of three different layers which are named as input layer, hidden layer, and output layer [95]. In this sense, an ANN can be considered as a hierarchical regression model.

In MPPT applications, ANN input variables can be selected as a combination of irradiance level, temperature level, open-circuit voltage, and short-circuit current of PV array. Then, in the hidden layer, which may involve more than one layer, neurons convert weighted input variables into proper outputs via an activation function such as sigmoid or tanh. Finally, ANN provides an estimated value for output voltage or output current of the PV array or duty cycle value, where this estimated value corresponds to GMPP. In indirect MPPT control applications, the estimated output is used as a reference for a controller or a perturbative method. In direct MPPT applications, estimated outputs are periodically generated and are applied to DC-DC converter directly. A typical three-layer ANN structure for MPPT application is shown in Fig. 10.

Tuning of the ANN weights requires heavy training which is another complex optimization problem. ANN weights are usually optimized via a long learning process, which can last for days or weeks, based on a feedback approach. Additionally, ANN needs different training for each PV cell model and array topology. However, a well-trained ANN-based MPPT model can provide highly accurate GMPP estimates. Further, using a higher number of neurons in the hidden layer increases the accuracy of the estimates, whereas it also increases computational time in the GMPPT process as a trade-off. Some of the related studies on ANN-based MPPT algorithms are reviewed in Table 10.

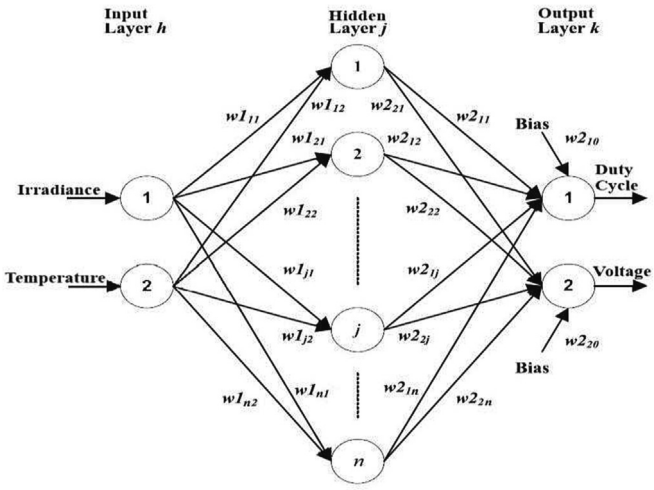

Fig. 10. Typical three-layer ANN-based MPPT structure.

4.4. Genetic algorithm

Genetic Algorithms refer to an AI-based bio-inspired evolutionary modeling technique that was developed based on J. H. Holland's studies in the 1960 s [104]. GA is mostly used as a metaheuristic optimizer or a classifier by mimicking evolution and natural selection processes that occur in the natural world. GA has three mechanisms which consist of a selection process based on the rule of survival of the fittest, and two reproduction processes based on crossing over and mutation of the genes. First, inputs are defined as the initial population which is represented by chromosomes. Then, a selection is performed according to fitness or objective function. After that, an intermediate population is created by randomly combined genes which are generated via reproduction mechanisms. Selection and reproduction processes are repeated until to reach the final population that corresponds to the optimal solution.

GAs are rarely used as an MPPT technique alone, rather employed in hybrid MPPT methods. The addition of GA increases tracking response characteristics and decreases SS oscillations under dynamic conditions. Also, GAs are able to find GMPP under PSC. Due to these advantages, GAs are combined with FLC, ANN, or conventional MPPT methods as well. However, implementation complexity and processing requirements can be considered disadvantages of GA-based MPPT methods. A flowchart for the general GA-based MPPT algorithm is presented in Fig. 11, and a literature review for related works on GA-based MPPT algorithms are provided in Table 11.

4.5. Swarm intelligence algorithms

Swarm Intelligence refers to collective and collaborative behavior of distributed and communicating multi-agent systems which can be natural or artificial. SI algorithms are metaheuristic optimizer methods which are inspired by behaviors of swarms of various species. These methods operate a collaborative search in a bounded search space via the agents of the swarm. In general, agents of the swarm follow simple rules during the search action. They may operate local searches, interact with other agents, and contribute to collective and collaborative behavior of the swarm.

SI algorithms can provide instantaneous solutions while continuing to search action. Even though, as metaheuristic algorithms, SI algorithms cannot guarantee the optimal solution, they usually show fast convergence to a near-optimal solution if it is not the

Table 10
Literature review on ANN-based MPPT algorithms.

Author(s)	Year	Method	Control Variable	Converter/ Processor	Application/Test(s)	Notes and Results
Rai et al. [96]	2011	ANN with optimal controller	Duty cycle	Buck-boost converter	Standalone system/ Simulation	Given irradiance, temperature, and wind speed as inputs to estimate MPP voltage and current. Employed optimal controller for MPP tracking. Outperformed PID.
Boumaaraf et al. [97]	2015	FLC-tuned ANN	Duty cycle	Buck-boost converter, Inverter	Grid-connected system/Simulation	Took irradiance, temperature, PV open-circuit voltage, and short-circuit current as inputs, to estimate MPP. Implemented with multi-level inverter. was provided. Able to track MPP under varying irradiance and temperature.
Arulmurugan and Suthanthiravanitha [98]	2015	FLC-based Hopfield NN	Duty cycle	Buck-boost converter/DSP	Standalone system/ Simulation, Prototype	Used PV output voltage and current as inputs, to predict MPP. Adapted step-sizes via FLC. Able to track effectively under changing conditions and PSC.
Messalti et al. [99,100]	2015, 2017	ANN with fixed and variable step-sizes	Duty cycle	Boost converter, Buck-boost converter/DSP	Standalone system/ Simulation, Prototype	Took PV output voltage and current as inputs and generated MPP estimates. Varied step-sizes according to change in PV output power. Provided fast response with less SS oscillations under rapidly changing conditions.
Du et al. [101]	2018	Hybrid fuzzy-weighted ELM with P&O	Duty cycle	Boost converter, Inverter	Grid-connected system/Simulation	Classified irradiance level via fuzzy-weighted extreme learning machine (ELM), an ANN with faster learning rate, to adapt step-sizes. Searched MPP by P&O. Performed with higher efficiency than traditional P&O.
Babes et al. [102]	2022	Hybrid ANN with ACO	Duty cycle	Boost converter, Inverter/DSP	Grid-connected system/Simulation, Hardware simulation	Tuned ANN based on PV output power via ACO. Used direct power control on inverter to compensate reactive power and reduce harmonics. Outperformed InC and ANN with faster convergence, less oscillation, and higher efficiency.
Haq et al. [103]	2022	ANN-based SMC	Voltage	Buck-boost converter	Standalone system/ Simulation	Employed ANN to generate reference voltage for SMC. Tracked GMPP with faster convergence and higher efficiency than SMC under various conditions.

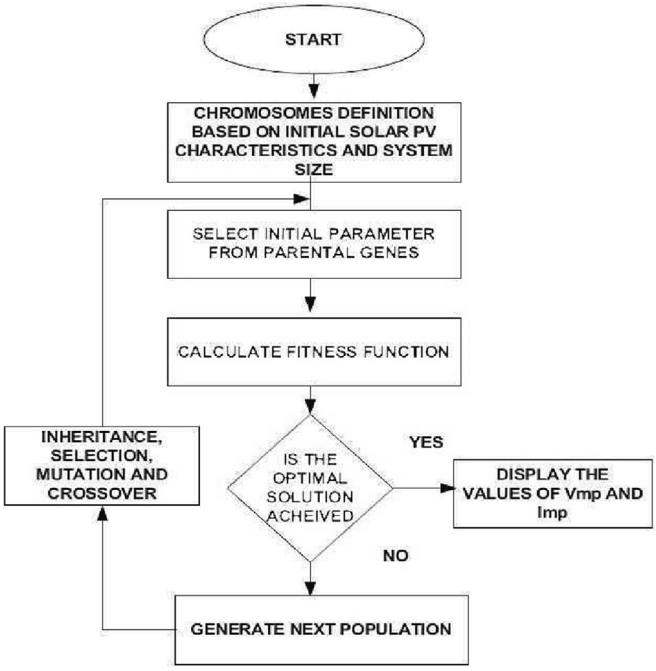

Fig. 11. General GA-based MPPT algorithm flowchart [8].

optimal. These methods also increase the probability of finding the global optimum among multiple extrema. Due to these advantages, SI algorithms have been increasingly employed as MPPT methods, particularly during the last decade. Ant Colony Optimization, Particle Swarm Optimization, Artificial Bee Colony, Firefly Algorithm, and many other recently developed SI algorithms will be covered in Section 4.5.1, Section 4.5.2, Section 4.5.3, Section 4.5.4, and Section 4.5.5 in order. Additionally, a chronologic literature review on SI-based MPPT algorithms will be provided at the end of Section 4.5.

4.5.1. Ant Colony optimization

Ant Colony Optimization is one of the first and most effective SI optimization algorithms that was proposed by M. Dorigo in 1991 [112]. ACO is a multi-agent probabilistic search algorithm that is inspired by the foraging behaviors of ant colonies. ACO is mostly utilized in combinatorial, stochastic, dynamic, and multi-objective optimization problems. Besides the discrete optimization problems, ACO also can be used in continuous or mixed optimization problems.

In ACO, artificial ants search for the minimum cost route to the food source via exchanging information with the colony. Information exchange is provided via pheromones released on the routes by the ants. Artificial ants find and gradually improve solutions by moving on the selected routes. Solutions evaluated with a probabilistic route selection based on pheromone amounts on the routes.

In ACO, at the end of each iteration, an ant, which has either the best solution in the iteration or the best solution since the start of the algorithm, updates the pheromone amounts as per (28), and also, each ant updates pheromone amounts on the last traversed route as shown in (29), where $\tau_{i,j}$ is the pheromone on route between i and j denoted by $R_{i,j}$, $\tau^*_{i,j}$ is updated pheromone, τ_0 is the initial pheromone, $\Delta\tau_{i,j}$ is defined as $1/L_{best}$ for the length of the best ant's path L_{best}, and q and r are constants in $(0,1]$ which corresponds to pheromone decay coefficient and pheromone evaporation rate, respectively. Each ant k selects its new route based on the likelihood $p^k_{i,j}$ which is calculated as seen in (30) where $\eta_{i,j}$ is inverse of the length of route$_{i,j}$, l denotes the destinations which is not yet visited, and α and β are control parameters to specify the relative effects of pheromone amounts and heuristic information, respectively.

$$\tau^*_{i,j} = \begin{cases} (1-r)\tau_{i,j} + r\cdot\Delta\tau_{i,j}, & \text{if } R_{i,j} \text{ is in the best path} \\ \tau_{i,j}, & \text{otherwise} \end{cases} \tag{28}$$

$$\tau^*_{i,j} = (1-q)\tau_{i,j} + q\tau_0 \tag{29}$$

Table 11
Literature review on GA-based MPPT algorithms.

Author(s)	Year	Method	Control Variable	Converter/ Processor	Application/Test(s)	Notes and Results
Messai et al. [105]	2011	GA-optimized FLC	Duty cycle	Boost converter	Standalone system/ Simulation	Tuned FLC membership functions and inference rules by GA. Implemented on FPGA. Performed with faster responses and better SS stability than P&O.
Kulaksiz and Akkaya [106]	2012	GA-optimized ANN with PI controller	Duty cycle	Inverter/ DSP	Standalone system/ Simulation, Induction motor	Utilized GA to optimize ANN. Predicted GMPP voltage by ANN as reference for PI controller. PI controller regulated inverter frequency based on voltage to frequency ratio by varying frequency change step-sizes. Outperformed conventional methods.
Shaiek et al. [107]	2013	GA	Duty cycle	Boost converter	Standalone system/ Simulation	Used GA to optimize MPP voltage online. Able to find GMPP under PSC where P&O and InC failed. Performed with higher efficiency than P&O and InC, whereas they converged faster than GA under dynamic conditions.
Daraban et al. [108]	2014	Hybrid GA and P&O	Voltage	Buck converter/ Computer	Standalone system/ Simulation, Hardware simulation	Optimized MPP by GA. Searched GMPP via P&O with variable step-sizes. Sped up convergence and reached 97% efficiency overall under changing irradiance and PSC.
Mohamed et al. [109]	2017	Hybrid GA with FLC and P&O	Duty cycle	Ćuk converter/ DSP	Standalone system/ Simulation, Motor pump set	Optimized MPP voltage via GA. Utilized FLC in MPP adjacency, P&O otherwise. Used over-current protection for motor. Outperformed P&O and InC with faster convergence and higher SS efficiency under dynamic conditions.
Ali et al. [110]	2021	Hybrid GA with FLC and ANN	Duty cycle	Boost converter, Inverter	Grid-connected system/Simulation	Combined GA-based FLC with GA-based ANN into GA-FLC-ANN. Outperformed P&O, InC, GA-based FLC and PSO-based FLC in convergence speed and accuracy.
Yadav et al. [111]	2022	Hybrid GA with GWO	Duty cycle	Boost converter	Standalone system/ Simulation	Parallelized with Gray Wolf Optimizer (GWO) by switching in each iteration. Able to perform under PSC. Performed with faster responses than GA and GWO.

$$p_{i,j}^{k}\begin{cases}\dfrac{\tau_{i,j}^{\alpha}\eta_{i,j}^{\beta}}{\sum_{\forall R_{i,l}}\tau_{i,l}^{\alpha}\eta_{i,l}^{\beta}}, & \text{if } R_{i,j} \textit{ is feasible}\\ 0, & \textit{otherwise}\end{cases} \tag{30}$$

In ACO-based MPPT method, a set of voltage, current, or duty cycle values can be initialized as possible routes. Pheromone amounts released on these routes can be associated with the PV array output power which corresponds to the route. Thus, after a few iterations, the best operating point which corresponds to MPP can be determined. ACO-based MPPT methods are mostly used to track GMPP under PSC. The main advantage of the ACO-based MPPT method is its very fast GMPP convergence ability in a few iterations.

4.5.2. Particle swarm optimization

Particle Swarm Optimization is a generic SI algorithm which was proposed by J. Kennedy and R. Eberhart in 1995 [113]. Since PSO algorithm is a simplified analogy for a social model where it is inspired by social behaviors of actual swarms such as flock of birds and school of fish but provides the algorithm without using any metaphor; it can be considered as the most generalized, representative, and popular one among all SI algorithms. PSO can be easily utilized in linear or nonlinear continuous numerical optimization problems, and it is highly open to minor and major modifications. Therefore, the popularity of PSO has increased in the last decade and it is widely employed in applied sciences, particularly in engineering applications.

PSO performs a collective and collaborative random search in a bounded space via multiple randomly located artificial agents called particles that iteratively update and develop their locations; and thus, inherently converge to a good enough solution that is probably very close or equal to the optimal solution of a continuous optimization model. In the initialization step, a number of particles are spread into the search area, on their initial positions. The initial position of each particle inherently becomes its initial best position. The best of the best positions remembered by each particle is assigned as the global best position of the swarm. In each iteration, first, a velocity vector is calculated for each particle, then present positions of the particles are updated based on the calculated velocity vectors. Finally, the updated positions are compared to the objective function value. These iterations are continuously repeated either up to a predetermined maximum number of iterations or until the stopping criterion is satisfied. Stopping criterion can be selected as the change in the global best position or the objective function evaluated on it. If the optimum value exists, it will be found in the global best position at the end of the process.

Mathematical expressions for the velocity vector and the present position of the i^{th} particle, which are denoted by $v_{i,j}$ and $x_{i,j}$ respectively in the j^{th} iteration for $i \in \{1,2,\cdots,n\}$ and $j \in \{1,2,\cdots,j_{max}\}$, are calculated as per (31) and (32) where c_1 and c_2 are two positive scalars, r_1 and r_2 are two random variables which follow a uniform distribution within $[0,1]$, w is the inertia of each particle, $p_{best,i}$ is the best position remembered by i^{th} particle, g_{best} is the global best position for the swarm, n is number of particles.

$$v_{i,j} = w v_{i,j-1} + c_1 r_1 \left(p_{best,i} - x_{i,j-1}\right) + c_2 r_2 \left(g_{best} - x_{i,j-1}\right) \tag{31}$$

$$x_{i,j} = x_{i,j-1} + v_{i,j-1} \tag{32}$$

In MPPT application, each position can be considered as a voltage, current or duty cycle value, and the objective function can be selected as the output power of the PV array. Then, PSO will solve the maximization problem for the voltage, current, or duty cycle that corresponds to GMPP. A flowchart for the general PSO-based MPPT algorithm is given in Fig. 12.

PSO-based MPPT algorithm can provide fast response, rapid convergence, and good GMPP accuracy under constant, dynamic, or PS conditions. A higher number of initialized particles increases convergence speed, and GMPP accuracy of the PSO, whereas increases required process power as well. In this case, PSO algorithm can be implemented on a processor with high process power such as DSP and FPGA that can be costed high. Since PSO is a multi-agent search algorithm, it will be more convenient to select FPGA, which can process data very fast in parallel, as the processor.

4.5.3. Artificial bee colony

Artificial Bee Colony is a powerful and efficient SI optimization algorithm which was proposed by D. Karaboga in 2005 [114]. ABC is a bio-inspired multi-agent probabilistic search algorithm with a well-defined metaphor that is based on the intelligence of honey-

bee swarms. ABC is a very useful optimization tool to solve multi-dimensional and multi-modal optimization problems since it operates local, global, and random searches together via different searching mechanisms. Thus, ABC is capable of getting out of local optima, even for extreme cases in multi-modal problems and converging to global optimum very fast and efficiently.

ABC algorithm has three types of agents which are employed bees, onlooker bees, and scout bees. Employed bees operate a local search mechanism and evaluate nectar amounts of food sources. Onlooker bees perform a global search mechanism and make choices of food sources based on nectar amounts. Scout bees stand for random search mechanism and make nonroutine exploration for new food sources.

In ABC-based MPPT algorithm, the duty cycle can be considered as the position of a food source, and the output power of the PV array is selected as fitness (objective) function, which is evaluated on a duty cycle, where it can be considered as nectar amount. Then, ABC algorithm will solve the maximization problem for the duty cycle which corresponds to GMPP. Duty cycles are initialized as seen in (33), employed bees are placed on these duty cycles and produce modified duty cycles based on initialized ones as new candidate solutions as per (34), where D_i is generated i th duty cycle value for index $i \in \{1, 2, \cdots, n\}$, n is the maximum number of randomly initialized duty cycles, D_l and D_u are the lower and upper limits for duty cycle values in order, D_{i^*} is modified duty cycle which produced based on D_i for randomly selected index $k \in \{1, 2, \cdots, n\}$ and $i \neq k$, r and m are random variables which follow uniform distributions within $[0, 1]$ and $[-1, 1]$ respectively, and output power of the PV array $P_{PV,i}$ is the fitness function which corresponds to D_i. Then, $P_{PV,i}$ is compared with P_{PV,i^*} by an employed bee and if P_{PV,i^*} is greater than $P_{PV,i}$, then D_{i^*} will be used instead of D_i and D_i will be forgotten by the employed bee; otherwise, there will not be any change. After that, an onlooker bee makes a probabilistic selection based on the likelihood function f_i which is calculated for D_i as shown in (35), and algorithm iterated. Employed bees are placed on duty cycles again, and steps are repeated until the stopping criteria are reached. If there is no further improvement on D_i for number of iterations which equals to a predetermined limit, then D_i will be abandoned by the employed bee, and scout bee will generate a random duty cycle as per (33) instead of abandoned one and place her on it.

$$D_i = D_l + r(D_u - D_l) \tag{33}$$

$$D_{i^*} = D_i + m(D_i - D_k) \tag{34}$$

$$f_i = \frac{P_{PV,i}}{\sum_{k=1}^{n} P_{PV,k}} \tag{35}$$

ABC-based MPPT method is able to track GMPP with very high accuracy and very fast convergence dynamic condition and PSC. Also, ABC can provide effective MPPT with very small SS error; thus, it operates with very high efficiency. Implementation of ABC-based MPP algorithm requires high process power, and it can be implemented on a DSP or a high-power microcontroller.

4.5.4. Firefly algorithm

Firefly Algorithm is another powerful SI optimization algorithm which was proposed by X.-S. Yang in 2007 [115]. FA is a bio-inspired multi-agent stochastic search algorithm that is inspired by the flashing characteristic of fireflies. In FA, it is assumed that each firefly is attracted by other fireflies, based on their attractiveness that are proportional to their brightness and inversely proportional to distances to them. The brightness of each firefly is evaluated according to the objective function of the optimization model.

First, all fireflies are initialized on random locations in a bounded solution space, and their initial brightness are evaluated for their initial locations. Then, distance and attractiveness between each two fireflies are determined as per (36) and (37) respectively where $r_{i,j,h}$ and $\beta_{i,j,h}$ are distance and attractiveness between the i th and j th fireflies at h th iteration for $i, j \in \{1, 2, \cdots, n\}$, $k \in \{1, 2, \cdots, k_{max}\}$, $i \neq j$, $x_{i,h}$ and $x_{j,h}$ are the locations of fireflies i and j at h th iteration, $\beta_{i,h}$ is attractiveness of the firefly i at its origin $x_{i,h}$, γ is a constant absorption coefficient for the brightness, and n is the number of fireflies. Once attractiveness between each two fireflies is determined, for each firefly, a comparison is performed among other fireflies of which attractiveness are higher than its own attractiveness. Then, the firefly moves towards the firefly j^*, which has the highest relative attractiveness, according to (38) where α is a random scalar which follows uniform distribution within $[0, 1]$ and ϵ_i is a vector of random variables which follow uniform distribution within $[-0.5, 0.5]$.

$$r_{i,j,h} = \|x_{i,h} - x_{j,h}\| \tag{36}$$

$$\beta_{i,j,h} = \beta_{i,h} e^{-\gamma r_{i,j,h}^2} \tag{37}$$

$$x_{i,h+1} = x_{i,h} + \beta_{i,j,h}\left(x_{j^*,h} - x_{i,h}\right) + \alpha\epsilon_i \tag{38}$$

In FA-based MPPT method, duty cycles may be considered as locations of fireflies, and the output power of the PV array may be chosen as the objective function, which is evaluated on a duty cycle, where it corresponds to the brightness of fireflies. Thus, GMPP can be obtained via FA as the optimal solution for a maximization problem. FA-based MPPT algorithm is able to provide high speed convergence, very high GMPP accuracy, very small or zero SS error, and very high efficiency. FA can be implemented on DSP or high-power microcontroller.

4.5.5. Other swarm intelligence algorithms

There are many other popular SI algorithms – which have been adapted for GMPPT methods during the last decade – such as Glowworm Swarm Optimization (GSO), Cuckoo Search (CS), Gravitational Search Algorithm (GSA), Bat-inspired Algorithm (BA), Fireworks Algorithm (FWA), Grey Wolf Optimizer (GWO), Whale Optimization Algorithm (WOA), and Salp Swarm Algorithm (SSA). Additionally, there are much more other recently developed SI algorithms. Even though most of them may be considered as variants of well-known SI algorithms, particularly of PSO, with minor modifications and different metaphors, these algorithms are applicable for high performance GMPPT methods as well.

K. N. Krishnanand and D. Ghose presented GSO in 2006. GSO, which was inspired by the luminescence of glowworms as similar to FA, has a movement mechanism like PSO, but it differs in terms of the adaptive neighborhoods limited by sights of glowworms, and the probabilistic selection based on fitness values of neighbors for the direction of movement [116]. CS is a multi-agent random search algorithm that was developed by X.-S. Yang and S. Deb in 2009 and inspired by the parasitic breeding behavior of cuckoos [117]. GSA, which was introduced by E. Rashedi, H. Nezamabadi-pour, and S. Saryazdi in 2009, is a multi-agent random search algorithm like PSO where the movement strategy of agents is based on Newton's Law of Universal Gravity [118]. BA, which was proposed by X.-S. Yang in 2010, is another multi-agent random search algorithm with a PSO-like movement strategy that mimics the echolocation behavior of microbats [119]. Y. Tan and Y. Zhu released FWA, which was inspired by the explosion of fireworks in 2010. In FWA, the numbers and locations of the sparks generated by each explosion are obtained based on the evaluation of fitness, and the direction of movement is determined via probabilistic selection for each firework [120]. S. Mirjalili, S. M. Mirjalili, and A. Lewis intro-

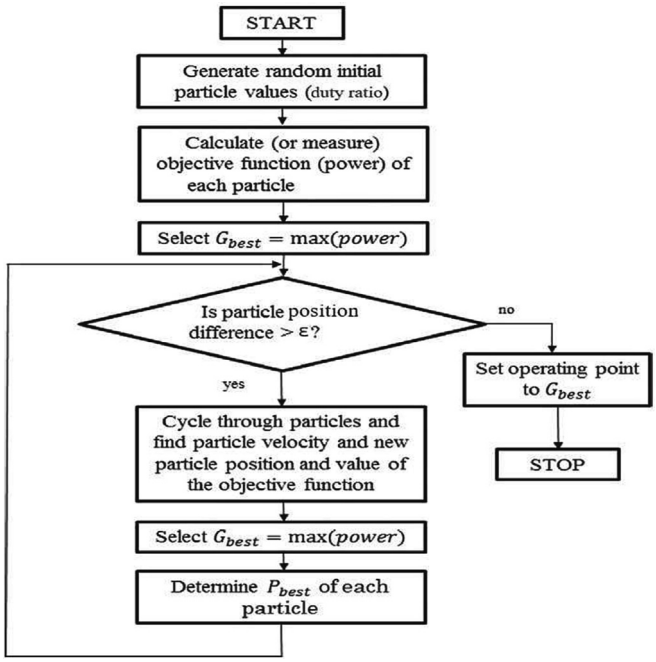

Fig. 12. General PSO-based MPPT algorithm flowchart [13].

duced GWO in 2014. GWO, which imitates the hierarchical group hunting behavior of grey wolves, has a movement mechanism based on the positions of three leading wolves and the distances of wolves from the prey, and a leader selection mechanism based on fitness function [121]. S. Mirjalili and A. Lewis also introduced WOA in 2016 with an inspiration of bubble-net hunting behavior of humpback whales. WOA employs a search mechanism that utilizes encircling strategy over shrinking spirals. [122]. S. Mirjalili et al. developed SSA in 2017. SSA, which is inspired foraging of salp chains, has a general movement mechanism based on simplified kinematic equation of displacement with acceleration where the leader of salp chain performs a convergent random movement. [123].

Table 12 presents a chronological literature review on SI-based MPPT algorithms.

5. Discussion

For choosing a proper MPPT method for a Solar PV system, MPPT methods should be evaluated in aspects of performance, implementation, and cost. According to this evaluation, the best-suited method, which is easy to implement, low-cost, and meets the requirements, can be chosen. In this section, a comparative overview in terms of performance, implementation, and cost of the MPPT methods, which are examined in Section 3 and Section 4 in detail, will be provided in a nutshell.

5.1. Conventional MPPT methods

Conventional MPPT methods provide direct control and are able to search MPP under constant and dynamic conditions; however, they are not capable of GMPPT under PSC. Conventional methods and their modified, adaptive, and hybridized versions with modern MPPT methods are still in use widely.

5.1.1. Perturbative methods

Perturbative methods such as P&O, InC, and HC are well-studied and widely used MPPT algorithms up to the present. The popularity of these methods continues since they can be simply implemented and easy to adapt due to their well-known algorithms. SS efficiency of fixed step-size perturbative methods is inversely proportional to step-size. Since larger step-size increases convergence speed, whereas increases SS oscillations as well, it decreases the MPP accuracy and efficiency. Since smaller step-size decreases convergence speed, therefore, even though the MPP accuracy and the SS efficiency increase, the overall efficiency of these methods decreases. With adaptive step-size perturbative methods, SS oscillations can be significantly decreased whereas converge speed slightly reduces, and thus better efficiencies can be achieved. Perturbative methods can find MPP with reasonable accuracy; however, none of these methods is capable of GMPPT under PSC, and their efficiencies decrease dramatically. When P&O, InC, and HC are compared with each other, contrary to popular belief that InC outperforms the others, it is revealed that there is no statistically significant difference between these methods [34,56]. In perturbative methods, one or two sensors are used, and they can be implemented on a low-cost microcontroller since they do not require complex calculations.

5.1.2. FOV and FSC methods

FOV and FSC MPPT methods may be preferred due to their simplicity and low-cost implementation. In these methods, an optimal proportionality constant needs to be determined according to the P-V characteristic of the PV array, and MPP is directly estimated based on the constant. Therefore, they can provide a fast response under dynamic conditions since they do not need any convergence; however, their MPP accuracies are low. Moreover, a power loss occurs during the measurement since the load is disconnected from the PV system. Therefore, efficiencies of these methods are low. Since the P-V characteristic of the PV array will change under PSC, these methods are not capable of GMPPT, and in this case, efficiency cannot be mentioned for these methods.

5.2. Modern MPPT methods

Modern MPPT methods can provide either direct or indirect control and are able to search MPP under constant and dynamic conditions. They are also highly capable of GMPPT under PSC. Modern MPPT methods and their modified and hybridized versions with conventional or other modern methods are popular due to their robust performances and still have been developing.

5.2.1. ACS-based methods

ACS-based methods such as well-known PID control and robust SMC are another commonly preferred approach for MPPT. However, the selection of parameters accurately is crucial for these methods, and this makes implementation relatively difficult. In these methods, a reference value obtained by other methods which are mostly conventional can be used. Also, they can be employed alone in MPPT applications; in that case, the slope of the P-V curve of the PV array is taken as an error. In ACS-based methods, SS errors converge to zero, and oscillations around the MPP are minimized. Thus, these methods have good MPP accuracies, convergence speeds, and very high SS efficiencies. Also, convergence speeds of ACS-based methods are high. However, both convergence speeds and efficiencies of controllers may decrease under fast changing conditions. These methods can track GMPP under PSC with small modifications. In these methods, besides the output voltage and current of the PV array, the output voltage and current of the converter can also be measured; therefore, two to four sensors are employed in general. If the controller parameters are tuned offline, the algorithm can be implemented on a low-cost microcontroller. If online-tuning

Table 12
Literature review on SI-based MPPT algorithms.

Author(s)	Year	Method	Control Variable	Converter/ Processor	Application/Test(s)	Notes and Results
Chowdhury and Saha [124]	2010	Adaptive Perceptive PSO	Duty cycle	Buck converter/ µCU	Standalone system/ Simulation, Prototype	Used Adaptive Perceptive PSO, a variant that searches in space in higher dimension. Reached 97.7% SS efficiency under varios PSC, whereas PSO performed with 96.4%.
Miyatake et al. [125]	2011	PSO	Duty cycle	Boost converter/ DSP	Standalone system/ Simulation, Prototype	Optimized duty cycles of multiple converters in a multi-array PV system by PSO at once. Able to find GMPP even for complex PS patterns.
Liu et al. [11]	2012	PSO	Duty cycle	Boost converter/ DSP	Standalone system/ Simulation, Prototype	Reinitialized PSO when a change in PS pattern detected based on changes in PV output power. Reached 99.5% SS efficiency under various PSC.
Ishaque et al. [126]	2012	Modified PSO	Duty cycle	Buck-boost converter/ DSP	Standalone system/ Simulation, Prototype	Optimized duty cycle based on generated 3 points. Reinitialized PSO when a change in PV output power occurred. Able to perform under PSC and fast changing irradiance. Eliminated SS oscillation and outperformed HC.
Ishaque and Salam [127]	2013	Hybrid PSO and HC	Duty cycle	Buck-boost converter/ DSP	Standalone system/ Simulation, Prototype	Integrated a HC-based local mode into [126] for direct duty cycle control. Able to track GMPP even under extreme PSC. Reached 99.5% SS efficiency in a 10-hour test.
Jiang et al. [128]	2013	ACO	Current	Not specified	Standalone system/ Simulation	Handled PSC by finding local MPPs for each string in PV array. Reinitialized when a change occurred in a PV string output current. Able to reach 99.9% SS efficiency under various PSC. Outperformed P&O but showed similar performance with PSO.
Sundareswaran et al. [129]	2014	FA	Duty cycle	Boost converter/ µCU	Standalone system/ Simulation, Prototype	Applied direct duty cycle according to optimized GMPP. Reinitialized FA when irradiance suddenly changed. Outperformed P&O with 99.99% SS efficiency and PSO in tracking speed and under PSC.
Ahmed and Salam [130]	2014	Hybrid CS with PID	Duty cycle	Buck-boost converter/ Computer	Standalone system/ Simulation, Hardware simulation	Optimized MPP by CS based on changes in PV output power. Used PID controller for smooth voltage transition. Performed faster and more accurate P&O and PSO under PSC.
Benyoucef et al. [131]	2015	ABC	Duty cycle	Boost converter/ DSP	Standalone system/ Simulation, Prototype	Used duty cycle corresponding to MPP optimized by ABC based on sudden PV output power changes. Outperformed PSO with 98.5–99.8% accuracies under various PSC.
Sundareswaran et al. [132]	2015	ABC	Duty cycle	Boost converter/ µCU	Standalone system/ Simulation, Prototype	Applied duty cycle corresponding to MPP optimized by ABC based on changes in PV output power, voltage and current. Obtained 99.2–100% SS efficiencies under 6 PSCs. Outperformed PSO with faster convergence and higher efficiency.
Sundareswaran et al. [133]	2015	Hybrid PSO and P&O	Duty cycle	Boost converter/ µCU	Standalone system/ Simulation, Prototype	Optimized MPP via PSO based on sudden large PV output power changes. Used P&O around estimated GMPP adjacency. Reached 99.7% and 100% SS efficiencies under various PSCs. Outperformed P&O in efficiency and PSO with faster responses.
Sudhakar Babu et al. [134]	2015	Modified PSO	Duty cycle	Boost converter/ µCU	Standalone system/ Simulation, Prototype	Optimized MPP by PSO starting with initial 3 duty cycles determined analytically based on PV module and the load parameters. Obtained 98.5–99.7% SS efficiencies under 10 PSCs. Outperformed InC, HC, and PSO in efficiency, response speed, and robustness.
Sundareswaran et al. [135]	2016	Hybrid ACO and P&O	Duty cycle	Boost converter/ µCU	Standalone system/ Simulation, Prototype	Used ACO to optimize MPP and P&O for fine-tuning in estimated GMPP adjacency. Outperformed P&O with 99.9–100% SS efficiencies and ACO and PSO with faster responses under PSC.
de Oliveira et al. [136]	2016	PSO	Voltage	Inverter/ DSP	Grid-connected system/Simulation, Prototype	Provided a grid-connected implementation. Reached 99.9% SS efficiency which was higher than P&O while showing slower responses under PSC.
Teshome et al. [137]	2016	Modified FA	Duty cycle	Boost converter/ DSP	Standalone system/ Hardware simulation	Simplified FA by using average position of brighter fireflies instead of each individual one. Rose FA SS efficiency from 99.1% to 99.8% and response speed by 40%.
Mohanty et al. [138]	2016	GWO	Duty cycle	Boost converter/ DSP	Standalone system/ Simulation, Hardware simulation	Able to perform under different PSCs. Outperformed P&O with 99.9% SS efficiency and improved PSO faster responses.
Titri et al. [139]	2017	Modified ACO	Duty cycle	Boost converter	Standalone system/ Simulation	Modified selection and updating process of ACO. Outperformed P&O, FLC, ANN, PSO, and ACO under PSC, in terms of SS efficiency and convergence speed.
Koad et al. [140]	2017	Modified PSO	Duty cycle	Ćuk converter	Standalone system/ Simulation	Used a modified PSO similar to [126] with addition of Lagrangian interpolation step. Reached 98% and 100% efficiencies under PSC and dynamic conditions. Performed with higher SS efficiency and convergence speed than P&O, InC, and PSO.
Manickam et al. [141]	2017	Hybrid FWA and P&O	Duty cycle	Boost converter/ DSP	Standalone system/ Prototype	Find MPP by FWA based on PS detection via changes in PV conductance and output power. Used P&O for fine-tuning in estimated GMPP adjacency. Sped up convergence with higher accuracy and reduced oscillations.
Kaced et al. [142]	2017	BA with Random Walk	Duty cycle	Buck-boost converter/ FPGA	Standalone system/ Simulation, Prototype	Optimized MPP via BA based on PV output power changes. Used Random Walk around estimated GMPP. Outperformed P&O and PSO with 99.9% SS efficiency under PSC.
Soufi et al. [143]	2017	Hybrid PSO and FLC	Duty cycle	Boost converter	Standalone system/ Simulation	Optimized FLC membership functions via PSO. Able to track GMPP in extreme atmospheric conditions without SS error and

Table 12 (*continued*)

Author(s)	Year	Method	Control Variable	Converter/ Processor	Application/Test(s)	Notes and Results
						faster convergence than PSO and P&O.
Jin et al. [144]	2017	GSO	Duty cycle	Boost converter	Standalone system/ Simulation	Tested under various atmospheric conditions and PSC. Able to show fast convergence and high GMPP accuracy. Outperformed P&O and FOV in all test cases.
Sen et al. [145]	2018	Modified PSO	Duty cycle	Boost converter/ DSP	Standalone system/ Simulation, Hardware simulation	Modified PSO weight factor and acceleration coefficients by dividing with open-circuit voltage. Sped up convergence, reduced SS oscillations, and rose GMPTT accuracy and overall efficiency. Obtained over 99% tracking efficiency for all PSCs.
Li et al. [146]	2018	Modified GSA	Duty cycle	Boost converter	Standalone system/ Simulation	Improved GSA with adaptive Gravitational constant change factor and modified particle velocity updating formula. Outperformed PSO and GSA in convergence speed, GMPP accuracy, and overall efficiency under various dynamic conditions and PSC.
Pilakkat and Kanthalakshmi [147]	2019	Hybrid ABC and P&O	Duty cycle	Boost converter	Standalone system/ Simulation	Identified GMPP region by ABC based on irradiation changes. Utilized P&O for fine-tuning. Obtained 99.6–99.9% SS efficiencies under different PSCs. Outperformed P&O with less overshoots and higher accuracy, tracking speed, and efficiency.
Yang et al. [148]	2019	Leader-based SI algorithms	Duty cycle	Buck-boost converter/ DSP	Standalone system/ Simulation, Hardware simulation	Used leader-based MPPT method employing 5SI algorithms: PSO, ABC, GWO, Moth-flame Optimization (MFO), and WOA. Shared individual algorithms' info with leader in each iteration. Outperformed individual SI algorithms under various conditions and PSC.
Mirza et al. [149]	2020	SSA	Duty cycle	Boost converter/ DSP	Standalone system/ Simulation, Hardware simulation	Obtained 99.3% average efficiency. Provided faster convergence and higher efficiency than P&O, GA, PSO, CS, PSO-GSA, and Dragonfly algorithm under various PSC.
Tao et al. [150]	2021	Hybrid WOA and Pattern Search-based ANFIS with InC	Duty cycle	Boost converter, Inverter	Standalone system/ Simulation	Optimized ANFIS parameters via WOA and Pattern Search. Combined ANFIS with InC. Outperformed conventional methods and FLC in tracking efficiency, convergence speed, and SS oscillations under changing conditions.
Moghassemi et al. [151]	2022	Improved hybrid WOA and DE	Duty cycle	Boost converter, Inverter	Standalone system/ Simulation	Used WOA and Differential Evolution (DE) together to speed up responses under PSC. Employed DE for broad searching and WOA for local searching. Provided faster convergence than WOA, DE, and WOA-DE in various PSCs.

via AI-based control and optimization algorithms is used to track MPP with higher efficiency, higher-cost controllers such as DSP or FPGA are needed. Although ACS-based MPPT methods are more successful than conventional methods in terms of performance, they cost higher in general.

5.2.2. AI-based methods

FLC-based MPPT methods work like ACS-based methods, with the addition of fuzzy membership functions and inference rules. However, determining membership functions is a complex process and makes the implementation of FLC difficult. In FLC-based MPPT methods, the input is classified based on the membership functions, and then output is generated with a logic that is similar to a look-up table. FLC has high MPP accuracy, SS efficiency, and convergence speed. FLC can also track GMPP under PSC. FLC-based MPPT methods are usually employed by hybridizing with conventional MPPT methods. Also, membership functions of FLC may be auto tuned via optimization methods such as ANN, GA, and SI. Thus, convergence speed and GMPP accuracy can be increased. In FLC-based MPPT methods, one or two sensors are used. Tuning algorithms for membership functions and calculations for the interference rules require high process power; hence high-cost processors such as DSP or FPGA are needed for FLC-based MPPT methods.

ANN and GA methods are mostly used by hybridizing with FLC and conventional MPPT methods. Thus, GMPPT methods with high efficiency, convergence speed, and GMPP accuracy can be obtained. It is complicated to implement ANN algorithms due to model training periods that can last too long. GA can be easily implemented in comparison to ANN. In these methods, besides the usage of voltage and current sensors, it may be required to measure irradiance and temperature values. For the implementation of ANN and GA methods, high process power processors such as DSP, FPGA, or CPU must be employed. Therefore, ANN and GA are considered high-cost MPPT methods.

Along with ever-developing SI algorithms, the performance of MPPT methods employing these algorithms has increased gradually. Efficiencies, convergence speeds, and GMPP accuracies of SI-based MPPT methods are very high. Particularly, SI-based MPPT algorithms, which include hierarchical evaluation mechanisms such as ACO and ABC and the ones that use simplified math such as GWO and SSA may provide faster convergence than classical PSO-like SI-based MPPT methods [129,132,135,138,149]. Moreover, implementation and adaptation of these methods that are generalized by PSO, in a similar approach, are relatively straightforward. Typically, voltage and current sensors are employed together in these methods. Process power requirements of SI-based methods vary based on the chosen parameters. For obtaining higher performance, a high-cost processor with high process power such as DSP or FPGA is needed. Additionally, via employing perturbative methods in local MPPT based on reference GMPP found by the SI algorithms, process power requirement may get lowered, and thus, the obtained high performance SI-based hybrid MPPT method may be implemented on a low-cost microcontroller.

SI-based MPPT algorithms, which superseded GA and ANN before, have become more popular than all other MPPT methods recently. Most of SI algorithms are also used in MPPT applications in parallel right after their development. Where the current number of developed SI algorithms exceeded a hundred, it may be foreseen that SI-based MPPT algorithms will become more prevalent in the near future.

Table 13
Comparison of MPPT methods.

Method	Performance				Implementation		Cost
	Tracking Efficiency	MPP Accuracy	Convergence Speed	GMPPT Capability	Algorithm Complexity	Required Process Power	
P&O with fixed step-size	Medium	High to Low[#]	Slow to Very Fast[#]	No	Simple	Low	Low
P&O with variable step-size	High	High	Fast	No	Medium	Medium	Medium
InC with fixed step-size	Medium	High to Low[#]	Slow to Very Fast[#]	No	Medium	Medium	Medium
InC with variable step-size	High	High	Fast	No	Medium	Medium	Medium
HC with fixed step-size	Medium	High to Low[#]	Slow to Very Fast[#]	No	Simple	Low	Low
HC with variable step-size	High	High	Fast	No	Medium	Medium	Medium
FOV	Low	Low	Not applicable	No	Very Simple	Very Low	Low
FSC	Low	Low	Not applicable	No	Very Simple	Very Low	Low
FLC	High	High	Fast	Yes	Complex	High	Medium
FLC with online tuning	Very High	High	Fast	Yes	Very Complex	Very High	High
PID	High	High	Fast	Yes	Medium	Low	Medium
PID with online tuning	Very High	High	Fast	Yes	Complex	High	High
Fractional-order **PID**	Very High	Very High	Fast	Yes	Complex	High	High
SMC	High	High	Fast	Yes	Complex	High	High
ANN	High	Very High	Fast	Yes	Very Complex	Very High	High
GA	High	Very High	Fast	Yes	Complex	High	High
ACO	Very High	High	Very Fast	Yes	Complex	High	High
PSO	Very High	High	Fast	Yes	Medium	High	High
Modified PSO	Very High	Very High	Fast	Yes	Complex	Very High	High
ABC	Very High	Very High	Very Fast	Yes	Complex	High	High
FA	Very High	Very High	Fast	Yes	Complex	High	High
GSO	Very High	High	Fast	Yes	Complex	High	High
CS	Very High	High	Fast	Yes	Complex	High	High
GSA	Very High	Very High	Fast	Yes	Medium	High	High
BA	Very High	Very High	Fast	Yes	Complex	High	High
FWA	Very High	Very High	Fast	Yes	Medium	High	High
GWO	Very High	Very High	Very Fast	Yes	Medium	High	High
WOA	Very High	Very High	Fast	Yes	Complex	High	High
SSA	Very High	Very High	Very Fast	Yes	Medium	Medium	High

[#] While step-size is increasing from small to large.

5.3. General evaluation of MPPT methods

General evaluation of MPPT methods comes through comparisons over performance and capabilities, implementation requirements, and application cost. A general evaluation may give an intuition about what kind of MPPT methods can meet which type of needs by fitting in limitations. In this respect, a general evaluation of MPPT methods is helpful as a starting point in selecting a proper MPPT method for an application. On the other hand, each specific MPPT application is highly dependent on its implementation details including both in software and hardware side. The selection of a best-suited MPPT method for an application is directly related to the needs and limitations of the application. Therefore, a general evaluation of MPPT methods should not be regarded as a certain assessment. The selection of the best-suited MPPT method for an application requires an additional specific evaluation per the needs and limitations.

Comparison of various MPPT methods should also not be taken as a precise inference about the methods. Due to the nature of MPPT concept, it is essentially an optimization problem. Concordantly, each MPPT method employs an optimization algorithm or approach. Hence, MPPT methods are subject to no free lunch theorems for optimization [152]. This means that no MPPT method will be able to give the best results for all aspects in every application. Each MPPT method has its own strengths and weaknesses. For example, perturbative methods may provide faster convergence than most of the modern MPPT methods under uniform irradiance, however, they cannot guarantee accurate tracking under PSC. Yet, the majority of MPPT research papers that propose a new MPPT method, including many of the highly cited prestigious ones examined in this review, come up with a result that the proposed method just outperformed all the compared MPPT methods in all aspects and all test cases. These contradictory results may be obtained by either only including the comparisons with the MPPT methods that are outperformed by the proposed method or only applying tests for the specific cases in which the proposed method works better. A more reliable comparison of various MPPT methods requires a more general outlook rather than comparing a proposed method with a few selected MPPT methods for a few test cases.

A comparison of MPPT methods, which are encompassed in this study, with a general outlook on the aspects of performance, implementation, and cost is provided in Table 13.

6. Conclusion

This study categorically presents the fundamental approaches of more than twenty MPPT methods with their variations used in Solar PV systems, and usages, advantages, and disadvantages of them. Besides the commonly used MPPT methods, new MPPT algorithms, which have started to be used in recent years, are also encompassed. Detailed literature reviews, including significant studies for each MPPT method covered in this paper, are chronologically provided. In the literature reviews consisting of more than a hundred prestigious studies conducted over the last decade, basics and differences of the proposed method, implementation details, used hardware, and simulation and experiment results, including the performance of the proposed method and its comparison with other methods, are examined. Additionally, a general comparative evaluation of the encompassed methods is presented.

This study aims to be a guide that may be useful for interested consumers, producers, and researchers and shed light on the last decade of maximum power point tracking methods for photovoltaic systems. To guide the ones who may use or work on MPPT methods, which conduce to effective and efficient usage of Solar PV

systems, a comprehensive examination that enables to track the developments in MPPT methods during the last decade and shows the current orientation and hotspots in the field is introduced.

Declaration of competing interest

The authors declare that they have no known competing financial interests or personal relationships that could have appeared to influence the work reported in this paper.

References

[1] IEA, "World Energy Outlook 2019," Paris, 2019.
[2] IAE, "World Energy Outlook 2022," Paris, 2022.
[3] S. Saravanan, N. Ramesh Babu, Maximum power point tracking algorithms for photovoltaic system - A review, Renew. Sustain. Energy Rev. 57 (2016) 192–204, https://doi.org/10.1016/j.rser.2015.12.105.
[4] A. Kumar, N. Gupta, V. Gupta, A comprehensive review on grid-TiedSolar Photovoltaic system, J. Green Eng. 7 (1) (2017) 213–254.
[5] K. Ishaque, Z. Salam, An improved modeling method to determine the model parameters of photovoltaic (PV) modules using differential evolution (DE), Sol. Energy 85 (9) (2011) 2349–2359, https://doi.org/10.1016/j.solener.2011.06.025.
[6] A.R. Jordehi, Maximum power point tracking in photovoltaic (PV) systems: A review of different approaches, Renew. Sustain. Energy Rev. 65 (2016) 1127–1138, https://doi.org/10.1016/j.rser.2016.07.053.
[7] K. Ishaque, Z. Salam, A review of maximum power point tracking techniques of PV system for uniform insolation and partial shading condition, Renew. Sustain. Energy Rev. 19 (2013) 475–488, https://doi.org/10.1016/j.rser.2012.11.032.
[8] J.P. Ram, T.S. Babu, N. Rajasekar, A comprehensive review on solar PV maximum power point tracking techniques, Renew. Sustain. Energy Rev. 67 (2017) 826–847, https://doi.org/10.1016/j.rser.2016.09.076.
[9] H. Islam, S. Mekhilef, N. Shah, T. Soon, M. Seyedmahmousian, B. Horan, A. Stojcevski, Performance evaluation of maximum power point tracking approaches and photovoltaic systems, Energies 11 (2) (2018) 365.
[10] F. Salem, M.A. Awadallah, Detection and assessment of partial shading in photovoltaic arrays, J. Electr. Syst. Inf. Technol. 3 (1) (2016) 23–32, https://doi.org/10.1016/j.jesit.2015.10.003.
[11] Y.H. Liu, S.C. Huang, J.W. Huang, W.C. Liang, A particle swarm optimization-based maximum power point tracking algorithm for PV systems operating under partially shaded conditions, IEEE Trans. Energy Convers. 27 (4) (2012) 1027–1035, https://doi.org/10.1109/TEC.2012.2219533.
[12] Y.H. Liu, J.H. Chen, J.W. Huang, A review of maximum power point tracking techniques for use in partially shaded conditions, Renew. Sustain. Energy Rev. 41 (2015) 436–453, https://doi.org/10.1016/j.rser.2014.08.038.
[13] S. Lyden, M.E. Haque, Maximum Power Point Tracking techniques for photovoltaic systems: A comprehensive review and comparative analysis, Renew. Sustain. Energy Rev. 52 (2015) 1504–1518, https://doi.org/10.1016/j.rser.2015.07.172.
[14] K. Ishaque, Z. Salam, Syafaruddin,, A comprehensive MATLAB Simulink PV system simulator with partial shading capability based on two-diode model, Sol. Energy 85 (9) (2011) 2217–2227, https://doi.org/10.1016/j.solener.2011.06.008.
[15] M.F.N. Tajuddin, M.S. Arif, S.M. Ayob, Z. Salam, Perturbative methods for maximum power point tracking (MPPT) of photovoltaic (PV) systems: A review, Int. J. Energy Res. 39 (9) (2015) 1153–1178, https://doi.org/10.1002/er.3289.
[16] N. Femia, G. Petrone, G. Spagnuolo, M. Vitelli, Optimization of perturb and observe maximum power point tracking method, IEEE Trans. Power Electron. 20 (4) (2005) 963–973, https://doi.org/10.1109/TPEL.2005.850975.
[17] A.K. Abdelsalam, A.M. Massoud, S. Ahmed, P.N. Enjeti, High-performance adaptive Perturb and observe MPPT technique for photovoltaic-based microgrids, IEEE Trans. Power Electron. 26 (4) (2011) 1010–1021, https://doi.org/10.1109/TPEL.2011.2106221.
[18] M. A. Elgendy, B. Zahawi, and D. J. Atkinson, "Evaluation of perturb and observe MPPT algorithm implementation techniques," in *IET Conference Publications*, 2012, vol. 2012, no. 592 CP, pp. 21–33. doi: 10.1049/cp.2012.0156.
[19] K. Ishaque, Z. Salam, G. Lauss, The performance of perturb and observe and incremental conductance maximum power point tracking method under dynamic weather conditions, Appl. Energy 119 (2014) 228–236, https://doi.org/10.1016/j.apenergy.2013.12.054.
[20] M.A.A. Mohd Zainuri, M.A. Mohd Radzi, A.C. Soh, N.A. Rahim, Development of adaptive perturb and observe-fuzzy control maximum power point tracking for photovoltaic boost dc-dc converter, IET Renew. Power Gener. 8 (2) (2014) 183–194, https://doi.org/10.1049/iet-rpg.2012.0362.
[21] S.K. Kollimalla, M.K. Mishra, A novel adaptive p&o mppt algorithm considering sudden changes in the irradiance, IEEE Trans. Energy Convers. 29 (3) (2014) 602–610, https://doi.org/10.1109/TEC.2014.2320930.
[22] M. Killi, S. Samanta, Modified perturb and observe MPPT algorithm for drift avoidance in photovoltaic systems, IEEE Trans. Ind. Electron. 62 (9) (2015) 5549–5559, https://doi.org/10.1109/TIE.2015.2407854.
[23] J. Ahmed, Z. Salam, An improved perturb and observe (P&O) maximum power point tracking (MPPT) algorithm for higher efficiency, Appl. Energy 150 (2015) 97–108, https://doi.org/10.1016/j.apenergy.2015.04.006.
[24] J. Ahmed, Z. Salam, A Modified P and O Maximum Power Point Tracking Method with Reduced Steady-State Oscillation and Improved Tracking Efficiency, IEEE Trans. Sustain. Energy 7 (4) (2016) 1506–1515, https://doi.org/10.1109/TSTE.2016.2568043.
[25] J. Ahmed, Z. Salam, An Enhanced Adaptive P&O MPPT for Fast and Efficient Tracking Under Varying Environmental Conditions, IEEE Trans. Sustain. Energy 9 (3) (2018) 1487–1496, https://doi.org/10.1109/TSTE.2018.2791968.
[26] R. Alik, A. Jusoh, Modified Perturb and Observe (P&O) with checking algorithm under various solar irradiation, Sol. Energy 148 (2017) 128–139, https://doi.org/10.1016/j.solener.2017.03.064.
[27] A.I.M. Ali, M.A. Sayed, E.E.M. Mohamed, Modified efficient perturb and observe maximum power point tracking technique for grid-tied PV system, Int. J. Electr. Power Energy Syst. 99 (December) (2018), https://doi.org/10.1016/j.ijepes.2017.12.029.
[28] M. Abdel-Salam, M.T. El-Mohandes, M. Goda, An improved perturb-and-observe based MPPT method for PV systems under varying irradiation levels, Sol. Energy 171 (February) (2018) 547–561, https://doi.org/10.1016/j.solener.2018.06.080.
[29] M. Kamran, M. Mudassar, M.R. Fazal, M.U. Asghar, M. Bilal, R. Asghar, Implementation of improved Perturb & Observe MPPT technique with confined search space for standalone photovoltaic system, J. King Saud Univ. - Eng. Sci. (2018), https://doi.org/10.1016/j.jksues.2018.04.006.
[30] G.A. Raiker, U. Loganathan, S. Reddy B., Current Control of Boost Converter for PV Interface With Momentum-Based Perturb and Observe MPPT, IEEE Trans. on Ind. Applicat. 57 (4) (2021) 4071–4079.
[31] A. I. M. Ali and H. R. A. Mohamed, "Improved P&O MPPT algorithm with efficient open-circuit voltage estimation for two-stage grid-integrated PV system under realistic solar radiation," *Int. J. Electr. Power Energy Syst.*, vol. 137, no. December 2021, p. 107805, May 2022, doi: 10.1016/j.ijepes.2021.107805.
[32] A. Safari, S. Mekhilef, Simulation and hardware implementation of incremental conductance MPPT with direct control method using cuk converter, IEEE Trans. Ind. Electron. 58 (4) (2011) 1154–1161, https://doi.org/10.1109/TIE.2010.2048834.
[33] Q. Mei, M. Shan, L. Liu, J.M. Guerrero, A novel improved variable step-size incremental-resistance MPPT method for PV systems, IEEE Trans. Ind. Electron. 58 (6) (2011) 2427–2434, https://doi.org/10.1109/TIE.2010.2064275.
[34] D. Sera, L. Mathe, T. Kerekes, S.V. Spataru, R. Teodorescu, On the perturb-and-observe and incremental conductance mppt methods for PV systems, IEEE J. Photovoltaics 3 (3) (2013) 1070–1078, https://doi.org/10.1109/JPHOTOV.2013.2261118.
[35] K.S. Tey, S. Mekhilef, Modified incremental conductance MPPT algorithm to mitigate inaccurate responses under fast-changing solar irradiation level, Sol. Energy 101 (2014) 333–342, https://doi.org/10.1016/j.solener.2014.01.003.
[36] T. Radjai, L. Rahmani, S. Mekhilef, J.P. Gaubert, Implementation of a modified incremental conductance MPPT algorithm with direct control based on a fuzzy duty cycle change estimator using dSPACE, Sol. Energy 110 (2014) 325–337, https://doi.org/10.1016/j.solener.2014.09.014.
[37] P. Sivakumar, A. Abdul Kader, Y. Kaliavaradhan, M. Arutchelvi, Analysis and enhancement of PV efficiency with incremental conductance MPPT technique under non-linear loading conditions, Renew. Energy 81 (2015) 543–550, https://doi.org/10.1016/j.renene.2015.03.062.
[38] R.I. Putri, S. Wibowo, M., Rifa'i,, Maximum power point tracking for photovoltaic using incremental conductance method, Energy Procedia 68 (2015) 22–30, https://doi.org/10.1016/j.egypro.2015.03.228.
[39] A. Loukriz, M. Haddadi, S. Messalti, Simulation and experimental design of a new advanced variable step size Incremental Conductance MPPT algorithm for PV systems, ISA Trans. 62 (2016) 30–38, https://doi.org/10.1016/j.isatra.2015.08.006.
[40] M.A. Elgendy, D.J. Atkinson, B. Zahawi, Experimental investigation of the incremental conductance maximum power point tracking algorithm at high perturbation rates, IET Renew. Power Gener. 10 (2) (2016) 133–139, https://doi.org/10.1049/iet-rpg.2015.0132.
[41] N.E. Zakzouk, M.A. Elsaharty, A.K. Abdelsalam, A.A. Helal, B.W. Williams, Improved performance low-cost incremental conductance PV MPPT technique, IET Renew. Power Gener. 10 (4) (2016) 561–574, https://doi.org/10.1049/iet-rpg.2015.0203.
[42] N. Kumar, I. Hussain, B. Singh, B.K. Panigrahi, Self-Adaptive Incremental Conductance Algorithm for Swift and Ripple-Free Maximum Power Harvesting From PV Array, IEEE Trans. Ind. Informatics 14 (5) (May 2018) 2031–2041, https://doi.org/10.1109/TII.2017.2765083.
[43] H. Shahid, M. Kamran, Z. Mehmood, M.Y. Saleem, M. Mudassar, K. Haider, Implementation of the novel temperature controller and incremental conductance MPPT algorithm for indoor photovoltaic system, Sol. Energy 163 (January) (2018) 235–242, https://doi.org/10.1016/j.solener.2018.02.018.
[44] S. Motahhir, A. El Ghzizal, S. Sebti, A. Derouich, Modeling of photovoltaic system with modified incremental conductance algorithm for fast changes of irradiance, Int. J. Photoenergy 2018 (2018) 1–13, https://doi.org/10.1155/2018/3286479.

[45] S. Necaibia, M.S. Kelaiaia, H. Labar, A. Necaibia, E.D. Castronuovo, Enhanced auto-scaling incremental conductance MPPT method, implemented on low-cost microcontroller and SEPIC converter, Sol. Energy 180 (October) (2019), https://doi.org/10.1016/j.solener.2019.01.028.
[46] J. Mishra, S. Das, D. Kumar, M. Pattnaik, A novel auto-tuned adaptive frequency and adaptive step-size incremental conductance MPPT algorithm for photovoltaic system, Int. Trans. Electr. Energy Syst. 31 (10) (Oct. 2021) 1–14, https://doi.org/10.1002/2050-7038.12813.
[47] E.M. Ahmed, H. Norouzi, S. Alkhalaf, Z.M. Ali, S. Dadfar, N. Furukawa, Enhancement of MPPT controller in PV-BES system using incremental conductance along with hybrid crow-pattern search approach based ANFIS under different environmental conditions, Sustain Energy Technol Assess 50 (2022) 101812.
[48] T. Esram, P.L. Chapman, Comparison of photovoltaic array maximum power point tracking techniques, IEEE Trans. Energy Convers. 22 (2) (2007) 439–449, https://doi.org/10.1109/TEC.2006.874230.
[49] M.A. Danandeh, S.M. Mousavi, Comparative and comprehensive review of maximum power point tracking methods for PV cells, Renew. Sustain. Energy Rev. 82 (November 2016) (2018) 2743–2767, https://doi.org/10.1016/j.rser.2017.10.009.
[50] F. Liu, Y. Kang, Y. Zhang, and S. Duan, "Comparison of P&O and hill climbing MPPT methods for grid-connected PV converter," in *2008 3rd IEEE Conference on Industrial Electronics and Applications*, Jun. 2008, pp. 804–807. doi: 10.1109/ICIEA.2008.4582626.
[51] E. Koutroulis, K. Kalaitzakis, N.C. Voulgaris, Development of a microcontroller-based, photovoltaic maximum power point tracking control system, IEEE Trans. Power Electron. 16 (1) (2001) 46–54, https://doi.org/10.1109/63.903988.
[52] W. Xiao and W. G. Dunford, "A modified adaptive hill climbing MPPT method for photovoltaic power systems," in *2004 IEEE 35th Annual Power Electronics Specialists Conference (IEEE Cat. No.04CH37551)*, 2004, pp. 1957–1963. doi: 10.1109/PESC.2004.1355417.
[53] S. A. Abuzed, M. P. Foster, and D. A. Stone, "Variable PWM step-size for modified Hill climbing MPPT PV converter," in *7th IET International Conference on Power Electronics, Machines and Drives (PEMD 2014)*, 2014, pp. 1957–1963. doi: 10.1049/cp.2014.0489.
[54] M. Lasheen, M. Abdel-Salam, Maximum power point tracking using Hill Climbing and ANFIS techniques for PV applications: A review and a novel hybrid approach, Energy Convers. Manag. 171 (March) (2018) 1002–1019, https://doi.org/10.1016/j.enconman.2018.06.003.
[55] C. Lohmeier, J. Zeng, W. Qiao, L. Qu, J. Hudgins, A current-sensorless MPPT quasi-double-boost converter for PV systems, in: 2011 IEEE Energy Conversion Congress and Exposition, 2011, pp. 1069–1075, https://doi.org/10.1109/ECCE.2011.6063892.
[56] S.B. Kjær, Evaluation of the hill climbing and the incremental conductance maximum power point trackers for photovoltaic power systems, IEEE Trans. Energy Convers. 27 (4) (2012) 922–929, https://doi.org/10.1109/TEC.2012.2218816.
[57] M. S. Bouakkaz, A. Boukadoum, O. Boudebbouz, I. Attoui, N. Boutasseta, and A. Bouraiou, "Fuzzy Logic based Adaptive Step Hill Climbing MPPT Algorithm for PV Energy Generation Systems," in *2020 International Conference on Computing and Information Technology (ICCIT-1441)*, Sep. 2020, pp. 1–5. doi: 10.1109/ICCIT-144147971.2020.9213737.
[58] J. Ahmad, "A fractional open circuit voltage based maximum power point tracker for photovoltaic arrays," in *2010 2nd International Conference on Software Technology and Engineering*, 2010, vol. 1, pp. 247–250. doi: 10.1109/ICSTE.2010.5608868.
[59] H.A. Sher, A.F. Murtaza, A. Noman, K.E. Addoweesh, K. Al-Haddad, M. Chiaberge, A New sensorless hybrid MPPT algorithm based on fractional short-circuit current measurement and P&O MPPT, IEEE Trans. Sustain. Energy 6 (4) (2015) 1426–1434, https://doi.org/10.1109/TSTE.2015.2438781.
[60] H.A. Sher, K.E. Addoweesh, K. Al-Haddad, An efficient and cost-effective hybrid MPPT method for a photovoltaic flyback microinverter, IEEE Trans. Sustain. Energy 9 (3) (2018) 1137–1144, https://doi.org/10.1109/TSTE.2017.2771439.
[61] C.C. Hua, Y.H. Fang, W.T. Chen, Hybrid maximum power point tracking method with variable step size for photovoltaic systems, IET Renew. Power Gener. 10 (2) (2016) 127–132, https://doi.org/10.1049/iet-rpg.2014.0403.
[62] H. Bounechba, A. Bouzid, H. Snani, A. Lashab, Real time simulation of MPPT algorithms for PV energy system, Int. J. Electr. Power Energy Syst. 83 (2016) 67–78, https://doi.org/10.1016/j.ijepes.2016.03.041.
[63] A. Hmidet, U. Subramaniam, R.M. Elavarasan, K. Raju, M. Diaz, N. Das, K. Mehmood, A. Karthick, M. Muhibbullah, O. Boubaker, L. Fara, Design of efficient off-grid solar photovoltaic water pumping system based on improved fractional open circuit voltage MPPT technique, Int. J. Photoenergy 2021 (2021) 1–18.
[64] H. Rezk, A.M. Eltamaly, A comprehensive comparison of different MPPT techniques for photovoltaic systems, Sol. Energy 112 (2015) 1–11, https://doi.org/10.1016/j.solener.2014.11.010.
[65] J.F. Silva, S.F. Pinto, Advanced control of switching power converters, in: Power Electronics Handbook, Elsevier, 2011, pp. 1037–1113, https://doi.org/10.1016/B978-0-12-382036-5.00036-7.
[66] B.N. Alajmi, K.H. Ahmed, S.J. Finney, B.W. Williams, Fuzzy-logic-control approach of a modified hill-climbing method for maximum power point in microgrid standalone photovoltaic system, IEEE Trans. Power Electron. 26 (4) (2011) 1022–1030, https://doi.org/10.1109/TPEL.2010.2090903.
[67] M. Adly, H. El-Sherif, and M. Ibrahim, "Maximum power point tracker for a PV cell using a fuzzy agent adapted by the fractional open circuit voltage technique," in *2011 IEEE International Conference on Fuzzy Systems (FUZZ-IEEE 2011)*, 2011, pp. 1918–1922. doi: 10.1109/FUZZY.2011.6007697.
[68] A. Al Nabulsi, R. Dhaouadi, Efficiency optimization of a DSP-based standalone PV system using fuzzy logic and dual-MPPT control, IEEE Trans. Ind. Inform. 8 (3) (2012) 573–584, https://doi.org/10.1109/TII.2012.2192282.
[69] Y.T. Chen, Y.C. Jhang, R.H. Liang, A fuzzy-logic based auto-scaling variable step-size MPPT method for PV systems, Sol. Energy 126 (2016) 53–63, https://doi.org/10.1016/j.solener.2016.01.007.
[70] S.D. Al-Majidi, M.F. Abbod, H.S. Al-Raweshidy, A novel maximum power point tracking technique based on fuzzy logic for photovoltaic systems, Int. J. Hydrogen Energy 43 (31) (2018) 14158–14171, https://doi.org/10.1016/j.ijhydene.2018.06.002.
[71] Y.-Y. Hong, A.A. Beltran, A.C. Paglinawan, A robust design of maximum power point tracking using Taguchi method for stand-alone PV system, Appl. Energy 211 (2018) 50–63.
[72] M. Bahrami, R. Gavagsaz-Ghoachani, M. Zandi, M. Phattanasak, G. Maranzanaa, B. Nahid-Mobarakeh, S. Pierfederici, F. Meibody-Tabar, Hybrid maximum power point tracking algorithm with improved dynamic performance, Renew. Energy 130 (2019) 982–991.
[73] O.F. Kececioglu, A. Gani, M. Sekkeli, Design and hardware implementation based on hybrid structure for MPPT of PV system using an interval Type-2 TSK fuzzy logic controller, Energies 13 (7) (2020) 1842, https://doi.org/10.3390/en13071842.
[74] R. Bisht, A. Sikander, An improved method based on fuzzy logic with beta parameter for PV MPPT system, Optik (Stuttg) 259 (March) (2022), https://doi.org/10.1016/j.ijleo.2022.168939.
[75] K.J. Åström, T. Hägglund, Revisiting the Ziegler-Nichols step response method for PID control, J. Process Control 14 (6) (2004) 635–650, https://doi.org/10.1016/j.jprocont.2004.01.002.
[76] J.G. Ziegler, N.B. Nichols, Optimum settings for automatic controllers, J. Dyn. Syst. Meas. Control 115 (2B) (Jun. 1993) 220–222, https://doi.org/10.1115/1.2899060.
[77] Z.L. Gaing, A particle swarm optimization approach for optimum design of PID controller in AVR system, IEEE Trans. Energy Convers. 19 (2) (2004) 384–391, https://doi.org/10.1109/TEC.2003.821821.
[78] D. Rekioua and E. Matagne, *Optimization of Photovoltaic Power Systems*. London: Springer London, 2012. doi: 10.1007/978-1-4471-2403-0.
[79] C.C. Chu, C.L. Chen, Robust maximum power point tracking method for photovoltaic cells: A sliding mode control approach, Sol. Energy 83 (8) (2009) 1370–1378, https://doi.org/10.1016/j.solener.2009.03.005.
[80] R. Xu, M. Zhou, Sliding mode control with sigmoid function for the motion tracking control of the piezo-actuated stages, Electron. Lett. 53 (2) (Jan. 2017) 75–77, https://doi.org/10.1049/el.2016.3558.
[81] A.I. Dounis, P. Kofinas, C. Alafodimos, D. Tseles, Adaptive fuzzy gain scheduling PID controller for maximum power point tracking of photovoltaic system, Renew. Energy 60 (2013) 202–214, https://doi.org/10.1016/j.renene.2013.04.014.
[82] Y. Levron, D. Shmilovitz, "Maximum power point tracking employing sliding mode control", *IEEE Trans*, Circuits Syst. I Regul. Pap. 60 (3) (2013) 724–732, https://doi.org/10.1109/TCSI.2012.2215760.
[83] E. Bianconi, J. Calvente, R. Giral, E. Mamarelis, G. Petrone, C.A. Ramos-Paja, G. Spagnuolo, M. Vitelli, A fast current-based MPPT technique employing sliding mode control, IEEE Trans. Ind. Electron. 60 (3) (2013) 1168–1178.
[84] E. Mamarelis, G. Petrone, G. Spagnuolo, Design of a sliding-mode-controlled SEPIC for PV MPPT applications, IEEE Trans. Ind. Electron. 61 (7) (2014) 3387–3398, https://doi.org/10.1109/TIE.2013.2279361.
[85] B.A. Kumar, M.S. Venkatesh, G.M. Muralikrishna, Optimization of photovoltaic power using PID MPPT controller based on incremental conductance algorithm, in: C. Kamalakannan, L.P. Suresh, S.S. Dash, B.K. Panigrahi (Eds.), Power Electronics and Renewable Energy Systems, vol. 326, Springer India, 2015, pp. 803–809, https://doi.org/10.1007/978-81-322-2119-7.
[86] A. Harrag, S. Messalti, Variable step size modified P&O MPPT algorithm using GA-based hybrid offline/online PID controller, Renew. Sustain. Energy Rev. 49 (2015) 1247–1260, https://doi.org/10.1016/j.rser.2015.05.003.
[87] A. Belkaid, J.P. Gaubert, A. Gherbi, An improved sliding mode control for maximum power point tracking in photovoltaic systems, Control Eng. Appl. Informatics 18 (1) (2016) 86–94.
[88] D.G. Montoya, C.A. Ramos-Paja, R. Giral, Improved design of sliding-mode controllers based on the requirements of MPPT techniques, IEEE Trans. Power Electron. 31 (1) (2016) 235–247, https://doi.org/10.1109/TPEL.2015.2397831.
[89] R. Pradhan, B. Subudhi, Double integral sliding mode MPPT control of a photovoltaic system, IEEE Trans. Control Syst. Technol. 24 (1) (Jan. 2016) 285–292, https://doi.org/10.1109/TCST.2015.2420674.
[90] B.o. Yang, T. Yu, H. Shu, D. Zhu, F. Zeng, Y. Sang, L. Jiang, Perturbation observer based fractional-order PID control of photovoltaics inverters for solar energy harvesting via Yin-Yang-Pair optimization, Energy Convers. Manag. 171 (2018) 170–187.
[91] M. Al-Dhaifallah, A.M. Nassef, H. Rezk, K.S. Nisar, Optimal parameter design of fractional order control based INC-MPPT for PV system, Solar Energy 159 (2018) 650–664.
[92] A. Nasir, I. Rasool, D. Sibtain, R. Kamran, Adaptive fractional order PID controller based MPPT for PV connected grid system under changing weather conditions, J. Electr. Eng. Technol. 16 (5) (2021) 2599–2610, https://doi.org/10.1007/s42835-021-00782-w.

[93] R.S. Inomoto, J.R.B.d.A. Monteiro, A.J.S. Filho, Boost converter control of PV system using sliding mode control with integrative sliding surface, IEEE J. Emerg. Sel. Top. Power Electron. 10 (5) (2022) 5522–5530.
[94] F. Rosenblatt, The perceptron: A probabilistic model for information storage and organization in the brain, Psychol. Rev. 65 (6) (1958) 386–408, https://doi.org/10.1037/h0042519.
[95] A.K. Jain, J. Mao, K.M. Mohiuddin, Artificial neural networks: a tutorial, Computer (Long Beach. Calif) 29 (3) (1996) 31–44, https://doi.org/10.1109/2.485891.
[96] A.K. Rai, N.D. Kaushika, B. Singh, N. Agarwal, Simulation model of ANN based maximum power point tracking controller for solar PV system, Sol. Energy Mater. Sol. Cells 95 (2) (2011) 773–778, https://doi.org/10.1016/j.solmat.2010.10.022.
[97] H. Boumaaraf, A. Talha, O. Bouhali, A three-phase NPC grid-connected inverter for photovoltaic applications using neural network MPPT, Renew. Sustain. Energy Rev. 49 (2015) 1171–1179, https://doi.org/10.1016/j.rser.2015.04.066.
[98] R. Arulmurugan, N. Suthanthiravanitha, Model and design of a fuzzy-based Hopfield NN tracking controller for standalone PV applications, Electr. Power Syst. Res. 120 (2015) 184–193, https://doi.org/10.1016/j.epsr.2014.05.007.
[99] S. Messalti, A. G. Harrag, and A. E. Loukriz, "A new neural networks MPPT controller for PV systems," in *IREC2015 The Sixth International Renewable Energy Congress*, Mar. 2015, pp. 1–6. doi: 10.1109/IREC.2015.7110907.
[100] S. Messalti, A. Harrag, A. Loukriz, A new variable step size neural networks MPPT controller: Review, simulation and hardware implementation, Renewable and Sustainable Energy Reviews 68 (2017) 221–233.
[101] Y. Du, K. Yan, Z. Ren, W. Xiao, Designing localized MPPT for PV systems using fuzzy-weighted extreme learning machine, Energies 11 (10) (2018) 1–10, https://doi.org/10.3390/en11102615.
[102] B. Babes, A. Boutaghane, N. Hamouda, A novel nature-inspired maximum power point tracking (MPPT) controller based on ACO-ANN algorithm for photovoltaic (PV) system fed arc welding machines, Neural Comput. Appl. 34 (1) (Jan. 2022) 299–317, https://doi.org/10.1007/s00521-021-06393-w.
[103] I.U. Haq, Q. Khan, S. Ullah, S.A. Khan, R. Akmeliawati, M.A. Khan, J. Iqbal, W. Yao, Neural network-based adaptive global sliding mode MPPT controller design for stand-alone photovoltaic systems, PLoS One 17 (1) (Jan. 2022) e0260480.
[104] J.H. Holland, Genetic Algorithms, Sci. Am. 267 (1) (1992) 66–73.
[105] A. Messai, A. Mellit, A. Guessoum, S.A. Kalogirou, Maximum power point tracking using a GA optimized fuzzy logic controller and its FPGA implementation, Sol. Energy 85 (2) (2011) 265–277, https://doi.org/10.1016/j.solener.2010.12.004.
[106] A.A. Kulaksiz, R. Akkaya, A genetic algorithm optimized ANN-based MPPT algorithm for a stand-alone PV system with induction motor drive, Sol. Energy 86 (9) (2012) 2366–2375, https://doi.org/10.1016/j.solener.2012.05.006.
[107] Y. Shaiek, M. Ben Smida, A. Sakly, M.F. Mimouni, Comparison between conventional methods and GA approach for maximum power point tracking of shaded solar PV generators, Sol. Energy 90 (2013) 107–122, https://doi.org/10.1016/j.solener.2013.01.005.
[108] S. Daraban, D. Petreus, C. Morel, A novel MPPT (maximum power point tracking) algorithm based on a modified genetic algorithm specialized on tracking the global maximum power point in photovoltaic systems affected by partial shading, Energy vol. 74, no. C (2014) 374–388, https://doi.org/10.1016/j.energy.2014.07.001.
[109] A.A.S. Mohamed, A. Berzoy, O.A. Mohammed, Design and Hardware Implementation of FL-MPPT Control of PV Systems Based on GA and Small-Signal Analysis, IEEE Trans. Sustain. Energy 8 (1) (2017) 279–290, https://doi.org/10.1109/TSTE.2016.2598240.
[110] M.N. Ali, K. Mahmoud, M. Lehtonen, M.M.F. Darwish, Promising MPPT Methods Combining Metaheuristic, Fuzzy-Logic and ANN Techniques for Grid-Connected Photovoltaic, Sensors 21 (4) (Feb. 2021) 1244, https://doi.org/10.3390/s21041244.
[111] K. Yadav, B. Kumar, J.M. Guerrero, A. Lashab, A hybrid genetic algorithm and grey wolf optimizer technique for faster global peak detection in PV system under partial shading, Sustain. Comput. Informatics Syst. vol. 35, no. May (Sep. 2022), https://doi.org/10.1016/j.suscom.2022.100770 100770.
[112] M. Dorigo, M. Birattari, T. Stutzle, Ant colony optimization, IEEE Comput. Intell. Mag. 1 (4) (Nov. 2006) 28–39, https://doi.org/10.1109/MCI.2006.329691.
[113] J. Kennedy and R. Eberhart, "Particle swarm optimization," in *Proceedings of ICNN'95 - International Conference on Neural Networks*, 1995, vol. 4, pp. 1942–1948. doi: 10.1109/ICNN.1995.488968.
[114] D. Karaboga, B. Basturk, A powerful and efficient algorithm for numerical function optimization: Artificial bee colony (ABC) algorithm, J. Glob. Optim. 39 (3) (2007) 459–471, https://doi.org/10.1007/s10898-007-9149-x.
[115] X.-S. Yang, Firefly Algorithm, in: X.-.-S. Yang (Ed.), Nature-Inspired Metaheuristic Algorithms, 2nd ed., Luniver Press, Frome, 2010, pp. 81–96.
[116] K.N. Krishnanand, D. Ghose, B. Prasad, Glowworm swarm based optimization algorithm for multimodal functions with collective robotics applications, Multiagent Grid Syst. 2 (3) (2006) 209–222.
[117] X.-S. Yang and Suash Deb, "Cuckoo Search via Lévy flights," in *2009 World Congress on Nature & Biologically Inspired Computing (NaBIC)*, 2009, pp. 210–214. doi: 10.1109/NABIC.2009.5393690.
[118] E. Rashedi, H. Nezamabadi-pour, S. Saryazdi, GSA: A Gravitational Search Algorithm, Inf. Sci. (Ny) 179 (13) (Jun. 2009) 2232–2248, https://doi.org/10.1016/j.ins.2009.03.004.
[119] X.-S. Yang, "A New Metaheuristic Bat-Inspired Algorithm," in *Studies in Computational Intelligence*, vol. 284, J. R. González, D. A. Pelta, C. Cruz, G. Terrazas, and N. Krasnogor, Eds. Berlin: Springer, Berlin, Heidelberg, 2010, pp. 65–74. doi: 10.1007/978-3-642-12538-6_6.
[120] Y. Tan and Y. Zhu, "Fireworks Algorithm for Optimization," in *Lecture Notes in Computer Science (including subseries Lecture Notes in Artificial Intelligence and Lecture Notes in Bioinformatics)*, vol. 6145, no. PART 1, Y. Tan, Y. Shi, and K. C. Tan, Eds. Berlin: Springer, Berlin, Heidelberg, 2010, pp. 355–364. doi: 10.1007/978-3-642-13495-1_44.
[121] S. Mirjalili, S.M. Mirjalili, A. Lewis, Grey Wolf Optimizer, Adv. Eng. Softw. 69 (Mar. 2014) 46–61, https://doi.org/10.1016/j.advengsoft.2013.12.007.
[122] S. Mirjalili, A. Lewis, The Whale Optimization Algorithm, Adv. Eng. Softw. 95 (May 2016) 51–67, https://doi.org/10.1016/j.advengsoft.2016.01.008.
[123] S. Mirjalili, A.H. Gandomi, S.Z. Mirjalili, S. Saremi, H. Faris, S.M. Mirjalili, Salp Swarm Algorithm: A bio-inspired optimizer for engineering design problems, Adv. Eng. Softw. 114 (Dec. 2017) 163–191, https://doi.org/10.1016/j.advengsoft.2017.07.002.
[124] S.R. Chowdhury, H. Saha, Maximum power point tracking of partially shaded solar photovoltaic arrays, Sol. Energy Mater. Sol. Cells 94 (9) (Sep. 2010) 1441–1447, https://doi.org/10.1016/j.solmat.2010.04.011.
[125] M. Miyatake, M. Veerachary, F. Toriumi, N. Fujii, H. Ko, Maximum power point tracking of multiple photovoltaic arrays: A PSO approach, IEEE Trans. Aerosp. Electron. Syst. 47 (1) (2011) 367–380, https://doi.org/10.1109/TAES.2011.5705681.
[126] K. Ishaque, Z. Salam, M. Amjad, S. Mekhilef, An improved particle swarm optimization (PSO)-based MPPT for PV with reduced steady-state oscillation, IEEE Trans. Power Electron. 27 (8) (2012) 3627–3638, https://doi.org/10.1109/TPEL.2012.2185713.
[127] K. Ishaque, Z. Salam, A deterministic particle swarm optimization maximum power point tracker for photovoltaic system under partial shading condition, IEEE Trans. Ind. Electron. 60 (8) (2013) 3195–3206, https://doi.org/10.1109/TIE.2012.2200223.
[128] L.L. Jiang, D.L. Maskell, J.C. Patra, A novel ant colony optimization-based maximum power point tracking for photovoltaic systems under partially shaded conditions, Energy Build. 58 (2013) 227–236, https://doi.org/10.1016/j.enbuild.2012.12.001.
[129] K. Sundareswaran, S. Peddapati, S. Palani, MPPT of PV systems under partial shaded conditions through a colony of flashing fireflies, IEEE Trans. Energy Convers. 29 (2) (2014) 463–472, https://doi.org/10.1109/TEC.2014.2298237.
[130] J. Ahmed, Z. Salam, A Maximum Power Point Tracking (MPPT) for PV system using Cuckoo Search with partial shading capability, Appl. Energy 119 (2014) 118–130, https://doi.org/10.1016/j.apenergy.2013.12.062.
[131] A.S. Benyoucef, A. Chouder, K. Kara, S. Silvestre, O.A. sahed, Artificial bee colony based algorithm for maximum power point tracking (MPPT) for PV systems operating under partial shaded conditions, Appl. Soft Comput. J. 32 (2015) 38–48.
[132] K. Sundareswaran, P. Sankar, P.S.R. Nayak, S.P. Simon, S. Palani, Enhanced Energy Output From a PV System Under Partial Shaded Conditions Through Artificial Bee Colony, IEEE Trans. Sustain. Energy 6 (1) (Jan. 2015) 198–209, https://doi.org/10.1109/TSTE.2014.2363521.
[133] K. Sundareswaran, V. Vignesh kumar, S. Palani, Application of a combined particle swarm optimization and perturb and observe method for MPPT in PV systems under partial shading conditions, Renew. Energy 75 (2015) 308–317.
[134] T. Sudhakar Babu, N. Rajasekar, K. Sangeetha, Modified Particle Swarm Optimization technique based Maximum Power Point Tracking for uniform and under partial shading condition, Appl. Soft Comput. J. 34 (2015) 613–624, https://doi.org/10.1016/j.asoc.2015.05.029.
[135] K. Sundareswaran, V. Vigneshkumar, P. Sankar, S.P. Simon, P., Srinivasa, Rao, Nayak,, and, S., Palani,, Development of an Improved P&O Algorithm Assisted Through a Colony of Foraging Ants for MPPT in PV System, IEEE Trans. Ind. Informatics 12 (1) (2016) 187–200, https://doi.org/10.1109/TII.2015.2502428.
[136] F.M. de Oliveira, S.A. Oliveira da Silva, F.R. Durand, L.P. Sampaio, V.D. Bacon, L. B.G. Campanhol, Grid-tied photovoltaic system based on PSO MPPT technique with active power line conditioning, IET Power Electron. 9 (6) (2016) 1180–1191, https://doi.org/10.1049/iet-pel.2015.0655.
[137] D.F. Teshome, C.H. Lee, Y.W. Lin, K.L. Lian, "A modified firefly algorithm for photovoltaic maximum power point tracking control under partial shading", *IEEE*, J. Emerg. Sel. Top. Power Electron. 5 (2) (2017) 661–671, https://doi.org/10.1109/JESTPE.2016.2581858.
[138] S. Mohanty, B. Subudhi, P.K. Ray, A new MPPT design using grey Wolf optimization technique for photovoltaic system under partial shading conditions, IEEE Trans. Sustain. Energy 7 (1) (2016) 181–188, https://doi.org/10.1109/TSTE.2015.2482120.
[139] S. Titri, C. Larbes, K.Y. Toumi, K. Benatchba, A new MPPT controller based on the Ant colony optimization algorithm for Photovoltaic systems under partial shading conditions, Appl. Soft Comput. J. 58 (2017) 465–479, https://doi.org/10.1016/j.asoc.2017.05.017.
[140] R.B.A. Koad, A.F. Zobaa, A. El-Shahat, A Novel MPPT Algorithm Based on Particle Swarm Optimization for Photovoltaic Systems, IEEE Trans. Sustain. Energy 8 (2) (2017) 468–476, https://doi.org/10.1109/TSTE.2016.2606421.
[141] C. Manickam, G.P. Raman, G.R. Raman, S.I. Ganesan, N. Chilakapati, Fireworks enriched P&O algorithm for GMPPT and detection of partial shading in PV systems, IEEE Trans. Power Electron. 32 (6) (2017) 4432–4443, https://doi.org/10.1109/TPEL.2016.2604279.

[142] K. Kaced, C. Larbes, N. Ramzan, M. Bounabi, Z., elabadine, Dahmane,, Bat algorithm based maximum power point tracking for photovoltaic system under partial shading conditions, Sol. Energy 158 (September) (2017) 490–503, https://doi.org/10.1016/j.solener.2017.09.063.
[143] Y. Soufi, M. Bechouat, S. Kahla, Fuzzy-PSO controller design for maximum power point tracking in photovoltaic system, Int. J. Hydrogen Energy 42 (13) (2017) 8680–8688, https://doi.org/10.1016/j.ijhydene.2016.07.212.
[144] Y. Jin, W. Hou, G. Li, X. Chen, A glowworm swarm optimization-based maximum power point tracking for photovoltaic/thermal systems under non-uniform solar irradiation and temperature distribution, Energies 10 (4) (2017) pp, https://doi.org/10.3390/en10040541.
[145] T. Sen, N. Pragallapati, V. Agarwal, R. Kumar, Global maximum power point tracking of PV arrays under partial shading conditions using a modified particle velocity-based PSO technique, IET Renew. Power Gener. 12 (5) (2018) 555–564, https://doi.org/10.1049/iet-rpg.2016.0838.
[146] L.L. Li, G.Q. Lin, M.L. Tseng, K. Tan, M.K. Lim, A maximum power point tracking method for PV system with improved gravitational search algorithm, Appl. Soft Comput. J. 65 (2018) 333–348, https://doi.org/10.1016/j.asoc.2018.01.030.
[147] D. Pilakkat and S. Kanthalakshmi, "An improved P&O algorithm integrated with artificial bee colony for photovoltaic systems under partial shading conditions," *Sol. Energy*, vol. 178, no. March 2018, pp. 37–47, 2019, doi: 10.1016/j.solener.2018.12.008.
[148] B.o. Yang, T. Yu, X. Zhang, H. Li, H. Shu, Y. Sang, L. Jiang, Dynamic leader based collective intelligence for maximum power point tracking of PV systems affected by partial shading condition, Energy Convers. Manage. 179 (2019) 286–303.
[149] A.F. Mirza, M. Mansoor, Q. Ling, B. Yin, M.Y. Javed, A Salp-Swarm Optimization based MPPT technique for harvesting maximum energy from PV systems under partial shading conditions, Energy Convers. Manag. 209 (February) (2020), https://doi.org/10.1016/j.enconman.2020.112625 112625.
[150] H. Tao, M. Ghahremani, F.W. Ahmed, W. Jing, M.S. Nazir, K. Ohshima, A novel MPPT controller in PV systems with hybrid whale optimization-PS algorithm based ANFIS under different conditions, Control Eng. Pract. 112 (April) (2021), https://doi.org/10.1016/j.conengprac.2021.104809.
[151] A. Moghassemi, S. Ebrahimi, S. Padmanaban, M. Mitolo, J.B. Holm-Nielsen, Two fast metaheuristic-based MPPT techniques for partially shaded photovoltaic system, Internat. J. Electric. Power Energy Syst. 137 (2022) 107567.
[152] D.H. Wolpert, W.G. Macready, No free lunch theorems for optimization, IEEE Trans. Evol. Comput. 1 (1) (1997) 67–82, https://doi.org/10.1109/4235.585893.